

# Simulation of crop growth and energy and carbon dioxide fluxes at different time steps from hourly to daily

Jing Wang,<sup>1,2</sup> Qiang Yu<sup>1\*</sup> and Xuhui Lee<sup>3</sup>

<sup>1</sup> Institute of Geographical Sciences and Natural Resource Research, Chinese Academy of Sciences, Beijing 100101, People's Republic of China

<sup>2</sup> Graduate School of the Chinese Academy of Sciences, Beijing, 100039, People's Republic of China

<sup>3</sup> School of Forestry and Environmental Studies, Yale University, New Haven, CT 06511, USA

## Abstract:

Understanding the exchange processes of energy and carbon dioxide (CO<sub>2</sub>) in the soil–vegetation–atmosphere system is important for assessing the role of the terrestrial ecosystem in the global water and carbon cycle and in climate change. We present a soil–vegetation–atmosphere integrated model (ChinaAgrosys) for simulating energy, water and CO<sub>2</sub> fluxes, crop growth and development, with ample supply of nutrients and in the absence of pests, diseases and weed damage. Furthermore, we test the hypotheses of whether there is any significant difference between simulations over different time steps. CO<sub>2</sub>, water and heat fluxes were estimated by the improving parameterization method of the coupled photosynthesis–stomatal conductance–transpiration model. Soil water evaporation and plant transpiration were calculated using a multilayer water and heat-transfer model. Field experiments were conducted in the Yucheng Integrated Agricultural Experimental Station on the North China Plain. Daily weather and crop growth variables were observed during 1998–2001, and hourly weather variables and water and heat fluxes were measured using the eddy covariance method during 2002–2003. The results showed that the model could effectively simulate diurnal and seasonal changes of net radiation, sensible and latent heat flux, soil heat flux and CO<sub>2</sub> fluxes. The processes of evapotranspiration, soil temperature and leaf area index agree well with the measured values. Midday depression of canopy photosynthesis could be simulated by assessing the diurnal change in canopy water potential. Moreover, the comparisons of simulated daily evapotranspiration and net ecosystem exchange (NEE) under different time steps indicated that time steps used by a model affect the simulated results. There is no significant difference between simulated evapotranspiration using the model under different time steps. However, simulated NEE produces large differences in the response to different time steps. Therefore, the accurate calculation of average absorbed photosynthetic active radiation is important for the scaling of the model from hourly steps to daily steps in simulating energy and CO<sub>2</sub> flux exchanges between winter wheat and the atmosphere. Copyright © 2007 John Wiley & Sons, Ltd.

**KEY WORDS** photosynthesis; transpiration; stomatal conductance; CO<sub>2</sub> flux; evapotranspiration; coupled model; diurnal variation; winter wheat; model

Received 16 August 2005; Accepted 21 March 2006

## INTRODUCTION

Weather is one of the main factors that control vegetation growth and development (Wolf, 1993; Goudriaan, 1996; Nonhebel, 1996; Hoogenboom, 2000; Mall *et al.*, 2004). Changes in vegetation biomass and leaf area may, in turn, exert a significant influence on the water and carbon cycle and on the climate system at different temporal and spatial scales (Charney, 1975; Dickinson and Henderson-Sellers, 1988; Lean and Rowntree, 1993, 1997; Dirmeyer and Shukla, 1994; Bonan, 1995; Dickinson, 1995; Dolman *et al.*, 1997; Xue, 1997). The observation and modelling of carbon dioxide (CO<sub>2</sub>), water vapour and energy fluxes are the basic methods for increasing our understanding of the biophysical and physiological elements that control the mechanistic interactions between vegetation and atmosphere, in which the Fluxnet provides a powerful platform (Baldocchi, 2003). Based on long-term

continuous measurements of carbon, water and energy fluxes, developing soil–vegetation–atmosphere transfer (SVAT) models to study vegetative–atmosphere interactions and feedback mechanisms, and implementing them to meso-scale models and general circulation models (GCMs), will be an important task for predicting climate change and to assess the influence that this has on vegetation dynamic changes.

In the past few decades, numerous SVAT models have been developed that describe energy and water exchanges between the soil, the vegetation and the atmosphere (e.g. Deardorff, 1978; Sellers *et al.*, 1986, 1996; Noilhan and Planton, 1989; Flerchinger *et al.*, 1989, 1991; Dawes and Hatton, 1993; Famiglietti and Wood, 1994; Braden, 1995; Braud *et al.*, 1995; Noilhan and Mahfouf, 1996; Dickinson *et al.*, 1998). Earlier SVAT models took account for the physical processes of water vapour transport, but they greatly simplified representations of reality (Verhoef and Allen, 2000), especially of vegetation components (e.g. Deardorff, 1978; Flerchinger *et al.*, 1989, 1991). BATS (Dickinson, 1984) and SiB (Sellers *et al.*, 1986) could accurately simulate the sensible and latent heat fluxes

\* Correspondence to: Qiang Yu, Institute of Geographical Sciences and Natural Resources Research, Chinese Academy of Sciences, No. 11A, Datun Road, Beijing 100101, People's Republic of China.  
E-mail: yuq@igsrr.ac.cn

exchange between the vegetation, soil and the atmosphere; however, they failed to include the biochemical processes in the soil–vegetation–atmosphere continuum. Frequently, leaf stomatal conductance was modelled by an empirical multi-factorial function of light intensity, air temperature, humidity, atmospheric CO<sub>2</sub> concentration and soil moisture (Jarvis, 1976; Avissar *et al.*, 1985) or by a fixed surface conductance for each type of vegetation.

Although the multi-factorial approach was used widely because it could effectively simulate stomatal conductance, the feedback mechanisms between photosynthesis and stomatal conductance and the response of stomatal conductance to CO<sub>2</sub> concentration are not represented in these models. Ball *et al.* (1987) and Collatz *et al.* (1991) linked leaf stomatal conductance with the rate of net photosynthesis and CO<sub>2</sub> concentration. Following this connection, a more physiological approach based on combined models of photosynthesis and stomatal conductance emerged (Harley and Baldocchi, 1995; Leuning, 1995; Jacobs *et al.*, 1996). Subsequently, improved parameterization of photosynthesis and leaf stomatal conductance began to be implemented in SVAT models (see Bonan (1996), Sellers *et al.* (1996), and Dickinson *et al.* (1998)). However, the leaf stomatal conductance model was applied under an ample supply of water conditions and needed to be modified when the plant and the soil were in the absence of water. Our current model includes the influence of plant and soil water content on the leaf stomatal conductance based on the above models.

Furthermore, earlier SVAT models treated the vegetation canopy and soil layers as one layer (Deardorff, 1978; Dickinson *et al.*, 1986)—in what was commonly termed the ‘Big-leaf’ model, which is described by the Penman–Monteith equation (Monteith, 1965). Big-leaf models have some limitations in their application for sparse or heterogeneous vegetations, whereas multilayer or multi-source models could be applied to these systems well (Shuttleworth and Wallace, 1985; Sellers *et al.*, 1986; Dolman, 1993; Kustas and Norman, 1999). In addition, although most current SVAT models that are used in GCMs already simulate the biophysical interactions between the vegetation and the atmosphere by treating the water and heat balances of the vegetation canopy and soil layers in a more complex and detailed manner, they do not model dynamic changes of vegetation. For example, the interannual and intra-annual variations of leaf-area index (LAI) are a model input in a land surface model (Bonan, 1996) and in a simple biosphere model (Sellers *et al.*, 1996); therefore, they do not describe the two-way feedback mechanism between vegetation and the atmosphere. In recent years, some modellers began to combine SVAT models and vegetation growth models (e.g. Cox *et al.*, 2000; Lu *et al.*, 2001; Tsvetinskaya *et al.*, 2001). However, these models were based on larger time and spatial scales, and our current model studies the biophysical and biochemical processes between vegetation and atmosphere under shorter time-scales.

On the other hand, although crop growth models tend to be more mechanistic and integrative than earlier empirical models, there are still some gaps between reality and model simplifications. For example, the process method of distinguishing the vegetation canopy and the soil layer should be different for specific vegetation types and climate condition. Crop growth models should be modified to reflect the advances in a process-based SVAT model. For homogeneous and closed-canopy or wet regions, single-layer models (such as the Penman equation (Penman, 1948), the Penman–Monteith equation (Monteith, 1965) and the Priestley–Taylor equation (Priestley and Taylor, 1972)) are suitable for calculating evapotranspiration. Furthermore, two-source or multi-sourced models are appropriate for application to heterogeneous and sparsely vegetative and arid rangelands (Waggoner and Reifsnnyder, 1968; Chen, 1984a; Shuttleworth and Wallace, 1985; Choudhury and Monteith, 1988; Noihan and Planton, 1989; Kustas, 1990; Shuttleworth and Gurney, 1990; Mihailovic and Ruml, 1996; Brenner and Incoll, 1997). For those regions at mid-latitudes, such as the North China Plain, the two-source and multi-sourced models were obviously more suitable. Moreover, most crop growth models calculate photosynthesis and evapotranspiration separately, whereas they are coupled through stomatal regulation (Collatz *et al.*, 1991; Harley *et al.*, 1992; Leuning, 1995; Nikolov *et al.*, 1995).

The time step of models and the time-scale of climate variables are extremely important to the accuracy of simulated results and the efficiency of models (Goudriaan and van Laar, 1994; Hoogenboom, 2000). Models with monthly climate data as model input resulted in large under- and over-estimates of yield (Nonhebel, 1994). Therefore, most crop growth models use daily input data and daily time steps, primarily because only daily climate data are available for convenience of application. However, many physiological and physical processes in SVAT models are based on shorter time-scales, e.g. a midday depression of photosynthesis and transpiration often takes place under water-stressed conditions (Tazaki *et al.*, 1980; Puech-Suanzes *et al.*, 1989; Hirasawa and Hsiao, 1999; Trivedi *et al.*, 2000) and the response between different processes is non-linear in the course of a day.

We present an integrated soil–vegetation–atmosphere model in conjunction with a crop model in this study. The objectives of our research are to develop a soil–vegetation–atmosphere integrated model to simulate energy, water and CO<sub>2</sub> fluxes between winter wheat and the atmosphere, based on long-term continuous field measurements; and to compare the simulated results of the model under different time steps from 30 min to 1 day.

## MODEL DESCRIPTION

The soil–vegetation–atmosphere integrated model (ChinaAgrosys) consists of three modules (Figure 1), i.e. soil,

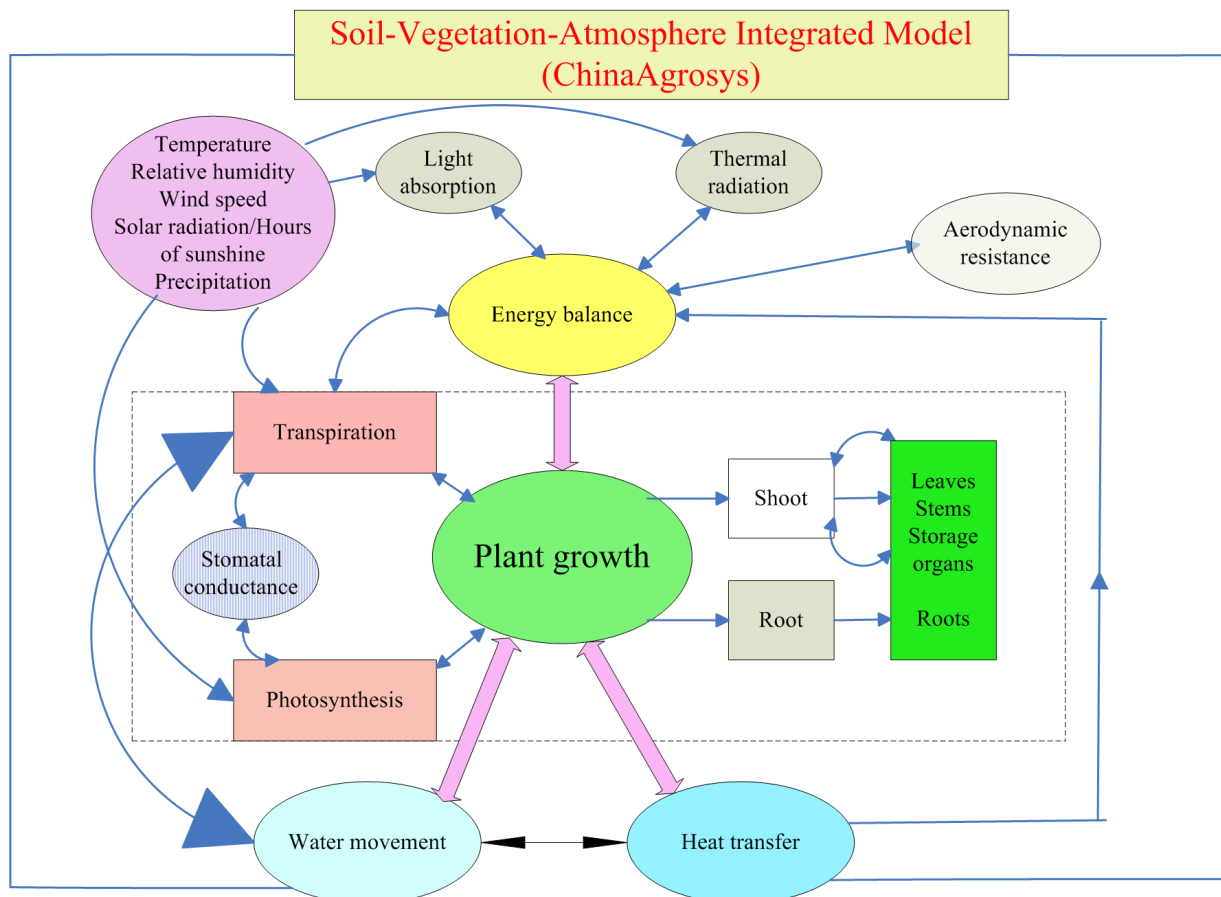


Figure 1. A schematic depiction of ChinaAgrosys

crop and microclimate. The soil module includes the heat transfer, water movement and root water uptake. The crop module includes submodels of photosynthesis and respiration, stomatal conductance, dry-matter partition, LAI and development. The microclimate module includes light distribution within the canopy, the energy balance and aerodynamic resistances, and canopy resistance. Leaf stomatal conductance is described using the combined photosynthesis–stomatal model, and the response of leaf stomatal conductance to leaf water potential is included. Canopy conductance is scaled up from the leaf by taking account of sunlit and sunshaded leaves. Soil water evaporation and plant transpiration were calculated using the multilayer water and heat transfer model with one soil layer and two vegetative layers.

#### Crop growth module

The crop growth module describes the photosynthesis and respiration of the canopy, photosynthate accumulation, dry-matter partitioning, the variation of LAI and phenological development. In the model, the photosynthesis and respiration of canopy and the variation of LAI are based on an instantaneous time-scale, whereas crop growth, dry-matter partitioning and phenological development are modelled based on a daily time-scale.

*Photosynthesis.* The canopy photosynthesis model is scaled up from the biochemical model of leaf photosynthesis (Farquhar *et al.*, 1980) by taking into account sunlit and sunshaded leaves. The gross photosynthetic rate  $P$  is expressed as a function of intercellular  $\text{CO}_2$  partial pressure  $P_i$ , photosynthetic photon flux density  $I$  and leaf temperature  $T_l$  (Collatz *et al.*, 1991):

$$P \approx \min \left\{ \begin{array}{l} J_E, f(I, a, P_i, T_l) \\ J_C, f(V_m, P_i, T_l) \\ J_S, f(T_l, V_m) \end{array} \right\} \quad (1)$$

in which  $J_E$  describes the response of photosynthesis to  $I$ ,  $J_C$  is the Rubisco-limited rate and  $J_S$  is the capacity for the export or utilization of the products of photosynthesis (usually sucrose synthesis). Based on the biochemical reaction of the Rubisco-limited rate, the relationship between photosynthesis and photon flux density  $I$  was represented by a non-rectangular hyperbola (Yu *et al.*, 2002):

$$\beta P^2 - P(\alpha I + P_{\max}) + \alpha I P_{\max} = 0 \quad (2)$$

in which  $\alpha$  is the initial photochemical efficiency,  $\beta$  is the convexity of the photosynthesis–light-response curve,  $P_{\max}$  is the maximal photosynthetic rate and  $P$  is the gross photosynthetic rate. The parameters  $\alpha$  and  $P_{\max}$  are related to the biochemical processes that are under the influence of environmental factors, the determinations

of which are referred to by Yu *et al.* (2002). Canopy photosynthesis  $P_c$  is the sum of photosynthesis of sunlit leaves and sunshaded leaves (Wang and Leuning, 1998):

$$P_c = P_{\text{sunlit}} + P_{\text{sunshaded}} \quad (3)$$

*Growth and respiration.* The growth rate of leaf, stem, root and grains is the net result of photosynthate accumulation and respiration losses. Maintenance respiration rate of leaf, stem, root and grains  $R_m$  is given by (Arora and Gajri, 2000)

$$R_m = R_{m0} W Q_{10}^{(T_a - T_o)/10} \quad (4)$$

$R_{m0}$  represents the maintenance respiration rates (mass of CH<sub>2</sub>O per kilogram of dry mass per hour) of leaf, stem, root and grains, which are set to 0.001 25 kg kg<sup>-1</sup> h<sup>-1</sup>, 0.000 625 kg kg<sup>-1</sup> h<sup>-1</sup>, 0.000 417 kg kg<sup>-1</sup> h<sup>-1</sup> and 0.000 417 kg kg<sup>-1</sup> h<sup>-1</sup> respectively, at the reference temperature ( $T_o = 25^\circ\text{C}$ ),  $W$  is the dry weight of leaf, stem, root and grains, and  $Q_{10}$  is the increment in respiration rate per 10°C temperature increment. In addition, about 10% of photosynthate is consumed in metabolic activity (Penning de Vries *et al.*, 1989; Arora and Gajri, 2000).

*Dry-matter partitioning.* Total dry-matter increase is partitioned between root and shoot, leaves, as well as stem and storage organs, according to the empirical partitioning coefficients that are based on observations in the North China Plain and other publications on winter wheat (Boons-Prins *et al.*, 1993).

*Phenological development.* The effects of temperature and photoperiod are considered in a phenological model of winter wheat, including vernalization. Phenological development is characterized by development stage, with values of zero at emergence, one at anthesis and two at maturity. Intermediate values are calculated according to the integrating development rate, which depends on the average air temperature and day length during the vegetative phase, and on the air temperature alone during the reproductive phase.

The development rate  $R_{\text{dev}}$  is calculated by a multiplicative function (Wang and Engel, 1998):

$$R_{\text{dev}} = R_{\text{dev,max}} f(T) f(V) f(h_{\text{php}}) \quad (5)$$

in which  $R_{\text{dev,max}}$  is the maximum development rate,  $f(T)$  is the temperature response function of the development rate, and  $f(V)$  and  $f(h_{\text{php}})$  represent the effects of vernalization and photoperiod respectively. A detailed description of these functions can be found in the paper by Wang and Engel (1998).

*Leaf-area index.* The variation in LAI is determined by the net growth rate; the death rate of leaves and water stress also decrease LAI, which is similar to the model of SUCROS (van Keulen *et al.*, 1982). The function used is

$$\text{LAI} = \text{SLAI}(\text{GLAI} - \text{RLAI}) \frac{\psi_c - \psi_w}{\psi_f - \psi_w} \quad (6)$$

in which SLAI (m<sup>2</sup> kg<sup>-1</sup>) is the specific leaf area, GLAI (kg m<sup>-2</sup> h<sup>-1</sup>) is the net growth rate of leaves, RLAI (kg m<sup>-2</sup> h<sup>-1</sup>) is the death rate of leaves due to leaf senescence after the flowering and shading effects in very dense canopies,  $\psi_c$  (hPa) is the canopy water potential,  $\psi_w$  (hPa) is the canopy wilting water potential, and  $\psi_f$  (hPa) is the maximal canopy water potential.

#### Microclimate

The microclimate module describes the transfer and distribution of solar radiation above and within the canopy, the energy and the water vapour exchange between the canopy, soil and the atmosphere. All these models are based on an instantaneous time-scale.

*Light distribution within canopy.* The global radiation consists of the direct visible and infrared radiation, and the diffuse visible and infrared radiation. The canopy is assumed to be homogeneous in a horizontal level; therefore, light intensity within the canopy decreases exponentially with LAI according to Beer's law. The extinction coefficient and canopy albedo for direct radiation and diffuse radiation are calculated separately according to Goudriaan (1977).

The leaves in the canopy are divided into sunlit and sunshaded leaves. The LAI of sunlit leaves is calculated according to the following expression (Wang and Leuning, 1998):

$$L_{\text{sunlit}} = \frac{1 - e^{-k_v(i)\text{LAI}}}{k_v(i)} \quad (7)$$

in which  $k_v(i)$  is the extinction coefficients for direct visible radiation,  $i = 1$  to 9, which denotes the inclination angles 0–10°, ..., 81–90° respectively. And the LAI of sunshaded leaves is

$$L_{\text{sunshade}} = \text{LAI} - L_{\text{sunlit}} \quad (8)$$

*Energy balance.* The energy balance equation of cropland not considering the effects of advection is given by

$$R_n = H + \lambda E + G \quad (9)$$

in which  $R_n$ ,  $H$ ,  $\lambda E$  and  $G$  are the net radiation above the canopy, the sensible heat flux above the canopy, the latent heat flux above the canopy and the soil heat flux respectively. Then, the energy balance equations of canopy and soil are expressed by

$$R_{\text{nc}} = H_c + \lambda E_c \quad (10)$$

$$R_{\text{ns}} = H_s + \lambda E_s + G \quad (11)$$

in which  $R_{\text{nc}}$  and  $R_{\text{ns}}$  are the net radiation absorbed by the canopy and the soil respectively,  $H_c$  and  $H_s$  are the sensible heat fluxes of the canopy and the soil respectively, and  $\lambda E_c$  and  $\lambda E_s$  are the latent heat fluxes of the canopy and the soil respectively. Sensible and latent

heat fluxes over the canopy and soil are described by the following expressions (Chen, 1984b):

$$H_c = \rho C_p \frac{(T_c - T_s)r_{a,1} + (T_c - T_a)(r_{a,2} + r_b^s)}{r_{a,1}(r_{a,2} + r_b^c + r_b^s) + r_b^c(r_{a,2} + r_b^s)} \quad (12)$$

$$H_s = \rho C_p \frac{(T_s - T_c)r_{a,1} + (T_s - T_a)r_b^c}{r_{a,1}(r_{a,2} + r_b^c + r_b^s) + r_b^c(r_{a,2} + r_b^s)} \quad (13)$$

$$\lambda E_c = \frac{\rho C_p}{\gamma} \frac{[e_s(T_c) - e_a](r_{a,2} + r_b^s + r_s^s) + [e_s(T_c) - e_s(T_s)]r_{a,1}}{r_{a,1}(r_{a,2} + r_b^c + r_b^s + r_s^s) + (r_b^c + r_s^c)(r_{a,2} + r_b^s + r_s^s)} \quad (14)$$

$$\lambda E_s = \frac{\rho C_p}{\gamma} \frac{[e_s(T_s) - e_a](r_b^c + r_s^c) + [e_s(T_s) - e_s(T_c)]r_{a,1}}{r_{a,1}(r_{a,2} + r_b^c + r_s^c + r_b^s + r_s^s) + (r_b^c + r_s^c)(r_{a,2} + r_b^s + r_s^s)} \quad (15)$$

in which  $\rho$  is air density,  $C_p$  is the specific heat at constant pressure,  $\lambda$  is the latent heat of vaporization,  $\gamma$  is the psychrometric constant,  $T_a$  is the air temperature at reference height,  $T_c$  is the canopy temperature,  $T_s$  is the soil surface temperature,  $r_{a,1}$  is the aerodynamic resistance from the middle part of the canopy to the reference height,  $r_{a,2}$  is the aerodynamic resistance from the bottom to the middle part of the canopy,  $r_b^c$  is the canopy surface boundary layer resistance,  $r_b^s$  is the soil surface boundary layer resistance,  $r_s^c$  is the canopy resistance, and  $r_s^s$  is the soil resistance.

*Aerodynamic resistances and canopy resistance.* How to determine the various resistances is the key to calculating sensible heat and latent heat fluxes. The resistances in the model include aerodynamic resistances, boundary-layer resistances of the canopy and soil, canopy resistance and soil resistance.

$$r_{a,1} = \frac{0.74 \left( \ln \left( \frac{z_r - d}{z_0} \right) - 2 \ln \left\{ \frac{1 + \sqrt{1 - 9[(z_r - d)/L]}}{2} \right\} - \ln \left( \frac{z_c - d}{z_0} \right) + 2 \ln \left\{ \frac{1 + \sqrt{1 - 9[(z_c - d)/L]}}{2} \right\} \right)}{ku_*} + r_{a,2} \quad (21)$$

Aerodynamic resistance is calculated according to the Monin and Obukhov similarity theory. Friction velocity  $u_*$  is defined, according to Goudriaan (1977), as

$$u_* = \frac{ku}{\ln \left( \frac{z_r - d}{z_0} \right) + 4.75 \frac{z_r - d}{L}} \quad (16)$$

in which  $k$  is von Karman's constant,  $z_r$  is the reference height,  $u$  is wind speed at the reference height,  $z_0$  is the roughness of the canopy,  $d$  is the zero-plane displacement, and  $L$  is the Monin–Obukhov length. When the atmospheric stratification is stable (Monin–Obukhov length  $L > 0$ ), the aerodynamic resistance from the middle part of the canopy to the reference height is calculated

by (Goudriaan, 1977)

$$r_{a,1} = \frac{0.74 \left[ \ln \left( \frac{z_r - d}{z_0} \right) + 4.7 \left( \frac{z_r - d}{L} \right) - \ln \left( \frac{z_c - d}{z_0} \right) - 4.7 \left( \frac{z_c - d}{L} \right) \right]}{ku_*} \frac{z_r - \frac{z_c}{2}}{z_r - z_c} \quad (17)$$

and the aerodynamic resistance from the middle part of the canopy to the soil surface is described by (Goudriaan, 1977)

$$r_{a,1} = \frac{0.74 \left[ \ln \left( \frac{z_r - d}{z_0} \right) + 4.7 \left( \frac{z_r - d}{L} \right) - \ln \left( \frac{z_c - d}{z_0} \right) - 4.7 \left( \frac{z_c - d}{L} \right) \right]}{ku_*} \frac{z_c/2}{z_r - z_c} \quad (18)$$

in which  $z_c$  is the crop height.

When the atmosphere is under unstable conditions (Monin–Obukhov length  $L < 0$ ), the aerodynamic resistance from the middle part of the canopy to the soil surface is expressed as (Goudriaan, 1977)

$$r_{a,2} = 0.37 \frac{z_c}{l_m} \frac{\exp(k_w/2) - 1}{k_w} \quad (19)$$

in which  $k_w$  is the extinction coefficient of wind speed by the canopy and  $l_m$  is the mean mixing length, which is given by (Goudriaan, 1977)

$$l_m = 1.2 \sqrt{4L_w z_c / \pi / LAI} \quad (20)$$

in which  $L_w$  is the average leaf width. Then, the aerodynamic resistance from the middle part of the canopy to the reference height is calculated by (Goudriaan, 1977)

Zero-plane displacement  $d$  is described by Monteith (1973) and roughness  $z_0$  is given by Goudriaan (1977):

$$d = 0.63z_c \quad (22)$$

$$z_0 = (z_c - d) \exp \left[ -\frac{z_c}{k_w(z_c - d)} \right] \quad (23)$$

The canopy boundary-layer resistance  $r_b^c$  and the soil boundary-layer resistance  $r_b^s$  can be calculated from the following expressions (Goudriaan, 1977):

$$r_b^c = \frac{90(L_w/u_{mid})^{1/2}}{L} \quad (24)$$

$$r_b^s = 180 \left( \frac{D_s}{u_s} \right)^{1/2} \quad (25)$$

in which  $D_s$  is the characteristic dimension of soil,  $u_{\text{mid}}$  is the wind speed in the middle part of the canopy, and  $u_s$  is the wind speed near the soil surface.

Canopy resistance is the reciprocal of canopy conductance to vapour:

$$r_s^c = \frac{1}{g_{\text{sw}}} \quad (26)$$

and canopy conductance is the sum of stomatal conductance of sunlit leaves and sunshade leaves:

$$g_s = g_{\text{sc, sunlit}} + g_{\text{sc, sunshaded}} \quad (27)$$

in which  $g_{\text{sc, sunlit}}$  and  $g_{\text{sc, sunshaded}}$  are calculated according to the coupled photosynthesis–stomatal-conductance model. The relationship between stomatal conductance to vapour  $g_{\text{sw}}$  and stomatal conductance to CO<sub>2</sub> is

$$g_{\text{sw}} = 1.6g_{\text{sc}} \quad (28)$$

Ball *et al.* (1987) proposed a semi-empirical stomatal model in which stomatal conductance  $g_s$  to CO<sub>2</sub> was expressed by relative humidity over leaf surface  $h_s$ , and CO<sub>2</sub> mole fraction  $C_s$  and net photosynthetic rate  $P_n$  under conditions of ample water supply:

$$g_s = g_{s0} + aP_n h_s / C_s \quad (29)$$

in which  $a$  is a constant and  $g_{s0}$  is the value of  $g_{\text{sc}}$  when the light is very weak. Leuning (1995) revised the Ball–Woodrow–Berry model by replacing the relative humidity over the leaf surface with leaf vapour pressure deficit VPD<sub>s</sub>:

$$g_s = m \frac{P_n}{(C_s - \Gamma)(1 + \text{VPD}_s / \text{VPD}_0)} + g_{s0} \quad (30)$$

in which VPD<sub>0</sub> is a parameter that reflects the characteristics of the response of stomata to atmospheric vapour pressure deficit (VPD),  $\Gamma$  is the CO<sub>2</sub> compensation point and  $m$  is an empirical regression parameter. Here, we introduce a limiting factor of leaf water potential on stomatal conductance,  $f(\psi_1)$ , and

$$g_s = m \frac{P_n}{(C_s - \Gamma)(1 + \text{VPD}_s / \text{VPD}_0)} f(\psi_1) + g_{s0} \quad (31)$$

in which  $f(\psi_1) = m_1[(\psi_1 - \psi_w)/(\psi_f - \psi_w)]$ .

The soil resistance in the model is estimated by the following expression (Lin and Sun, 1983):

$$r_s^s = a_1 \left( \frac{\theta_{\text{sc}}}{\theta_c} \right)^{b_1} + c_1 \quad (32)$$

in which  $\theta_{\text{sc}}$  is surface-saturated soil-water content,  $\theta_c$  is surface soil-water content, and  $a_1$ ,  $b_1$  and  $c_1$  are empirical constants.

### Soil

The soil module describes the transfer of water in the soil and the plant, heat transfer in the soil and determines the soil temperature and soil water content. These processes are based on an instantaneous time-scale.

*Heat and water transfer.* The vertical heat transfer in the non-saturated soil is simulated based on the equation of heat conduction:

$$c(z) \frac{\partial T_s}{\partial t} = \frac{\partial}{\partial z} \left( \lambda(z) \frac{\partial T_s}{\partial z} \right) \quad (33)$$

in which  $T_s$  is the soil temperature,  $c(z)$  is the specific heat and  $\lambda(z)$  is the thermal conductivity of the soil at depth  $z$ .

Soil water movement in the vertical direction is simulated based on the Richards equation:

$$c(\psi_s, z) \frac{\partial \psi_s}{\partial t} = \frac{\partial}{\partial z} \left( K(\psi_s, z) \frac{\partial \psi_s}{\partial z} \right) - \frac{\partial K(\psi_s, z)}{\partial z} - S(z, t) \quad (34)$$

in which  $c(\psi_s, z)$  is the water capacity of soil at depth  $z$ ,  $\psi_s$  is the soil water potential,  $K(\psi_s, z)$  is the water conductivity of soil at depth  $z$ , and  $S(z, t)$  is the root uptake rate.

In the model, basic equations of water and heat movement in the soil in the vertical direction are solved by the finite-difference method after initial conditions and boundary conditions are given.

*Root water uptake.* The calculation of root water uptake defines soil water distribution and plant transpiration. Hillel *et al.* (1976) developed a mechanistic model of root water uptake based on the water-flux equation (Van den Honert, 1948), which is expressed as

$$S(z, t) = \frac{\psi_s(z) - \psi_c}{R_s(z) + R_r(z) + R_x} \quad (35)$$

in which  $\psi_c$  is the canopy water potential,  $\psi_s(z)$  is the soil-water potential at the  $z$  layer,  $R_s(z)$  is the soil resistance to water current at the  $z$  layer,  $R_r(z)$  is root resistance at the  $z$  layer, and  $R_x$  is xylem resistance.

## MATERIALS AND METHODS

### Site description

Experiments on measuring water, heat and CO<sub>2</sub> fluxes, and the growth and development of winter wheat were conducted at the Yucheng Integrated Agricultural Experiment Station of Chinese Ecosystem Research Network (CERN), located on the North China Plain (36°40'N, 116°22'E, 28 m above average sea level). It has a temperate monsoon climate. The annual mean air temperature is 13.1 °C and the mean temperatures in January and July are −3 °C and +26.9 °C respectively. The mean annual precipitation is 610 mm and nearly 70% of precipitation is concentrated in summer. The soil type is a silty loam, with an average bulk density of 1.4 g cm<sup>−3</sup>. The cropping system in the region is a winter wheat–summer maize rotation. There was a fetch of more than 200 m for winds from all directions. Detailed descriptions of experimental conditions are given by Yu *et al.* (2002), Lee *et al.* (2004) and Wang *et al.* (2006).

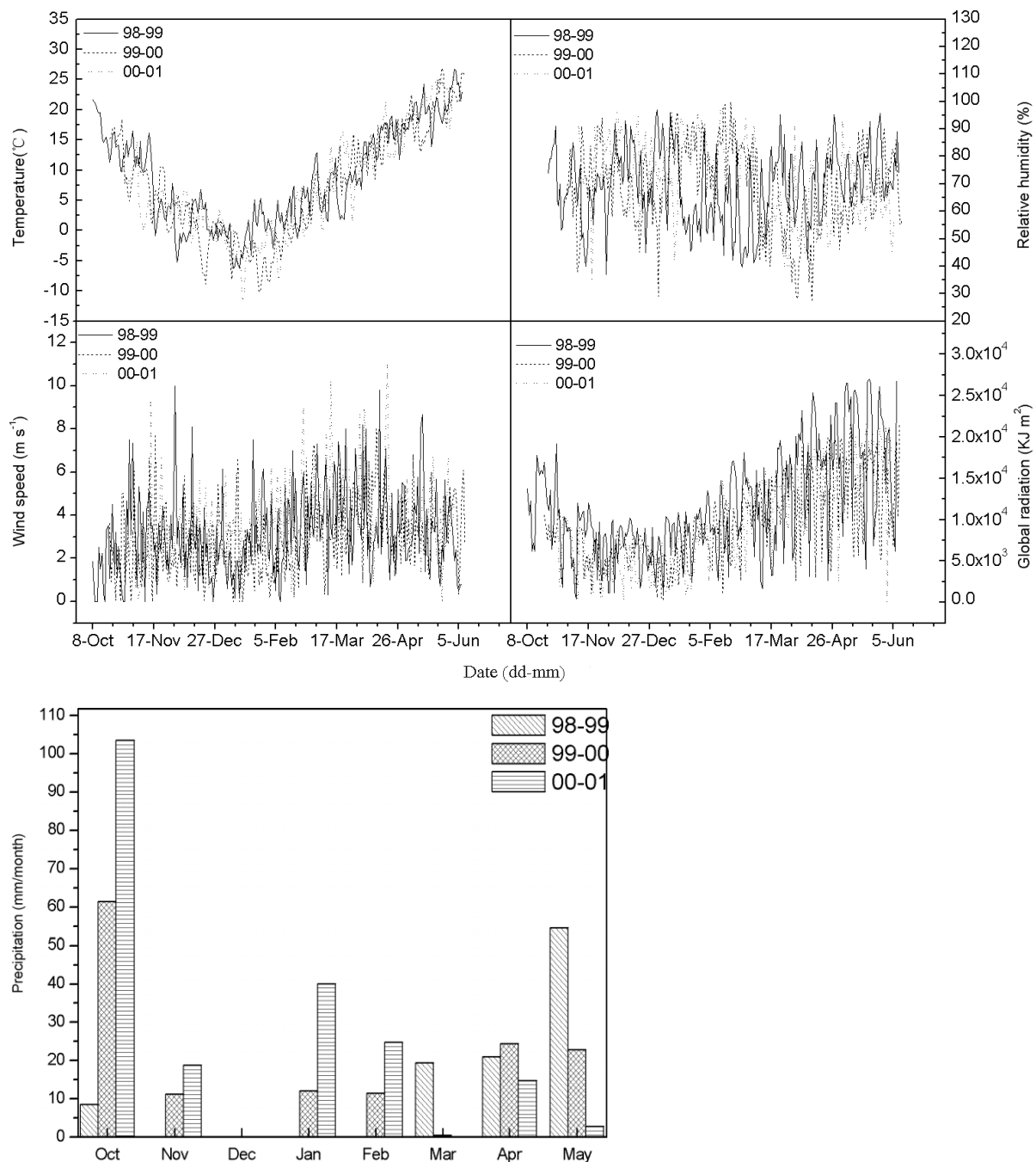


Figure 2. Seasonal variation of five meteorological factors, via daily average air temperature  $T$ , relative humidity  $RH$ , wind speed  $u$ , global radiation  $Q$  and precipitation  $P$  in three growing seasons of winter wheat in Yucheng (1998–2001)

### Field experiments

The experiment on measuring evapotranspiration, soil water content and the growth and development of winter wheat was conducted during three growing seasons of winter wheat in 1998–2001. The experiment on measuring water, heat and  $\text{CO}_2$  fluxes, and the growth and development of winter wheat was conducted in 2003.

**Meteorological factors.** Air temperature ( $^{\circ}\text{C}$ ), relative humidity (%), wind speed ( $\text{m s}^{-1}$ ) at a height of 2 m, sunshine hours (h), global radiation ( $\text{kJ m}^{-2}$ ) and precipitation ( $\text{mm day}^{-1}$ ) were collected by a meteorological observation system at Yucheng Station (Figure 2).

**Crop growth.** During each developmental stage, 20 plants were randomly harvested and plant density was counted in the field. The LAI was measured by a LICOR3100 instrument, and dry matter was weighed after the material of each component had been dried in an oven. At the end of the crop-growth season, the crops were harvested.

**Evapotranspiration and soil-water content.** Evapotranspiration was measured by a large weighing lysimeter, which has a surface area of  $3.14 \text{ m}^2$  and a depth of 5 m. A mechanical scale was used, which allowed reading of up to  $0.02 \text{ mm}$  of water loss. Measurements were taken at

Table I. Instruments and measurements for hourly meteorological variables and CO<sub>2</sub>, sensible and latent heat fluxes

Meteorological factors	Instrument	Company	Height of measurement (m)
Net radiation (W m <sup>-2</sup> )	Net radiometers (CNR-1)	Kipp & Zonen	1.86
Global radiation (W m <sup>-2</sup> )	Pyranometer (CM11)	Kipp & Zonen	1.86
Air temperature (°C)	Humidity probe (HMP45C)	VAISALA	2.05
Air relative humidity (%)	Humidity probe (HMP45C)	VAISALA	2.05
Wind speed (m s <sup>-1</sup> )	Anemometer (A100R)	Vector	2.05
Soil heat flux (W m <sup>-2</sup> )	Heat flux sensor (HFP01SC)	Hukseflux	0.05 below ground
Air pressure (hPa)	Barometer (CS105)	VAISALA	2.05
Soil temperature	Four thermocouple sensors (TCAV)	Campbell Scientific Ltd, Logan, UT, USA	0.02, 0.05, 0.10, 0.20, 0.50 below ground
Soil water content	Eight water content reflectometers (CS616.L)	Campbell Scientific	0, 0.05, 0.10, 0.15, 0.20, 0.40, 0.60, 1.00 below ground
CO <sub>2</sub> flux	CO <sub>2</sub> /H <sub>2</sub> O infrared analyser (Li-7500)	LI-COR	2.10
Sensible heat flux	Three-dimensional supersonic anemometer (CSAT3)	Campbell Scientific	2.10
Latent-heat flux	Three-dimensional supersonic anemometer (CSAT-3)	Campbell Scientific	2.10

08:00 and 20:00. Soil water was monitored using time-domain reflectometry (TDR) and recorded every 30 min at 0.15 m increments to a depth of 0.9 m. The TDR measurement was calibrated by soil-water content measured by an oven-dried method.

*Hourly meteorological factors and fluxes.* Hourly meteorological variables and water and heat fluxes were measured using an eddy covariance system (Table I). The position of eddy correlation equipment was 2.10 m above the ground; data were recorded using a datalogger (CR23X CSI) and the frequency of sampling was 20 Hz for each channel. The average values were calculated and recorded every 30 min. Though the eddy covariance method was thought to be the most accurate method for measuring water, heat and CO<sub>2</sub> fluxes at present, there were still significant problems in flux measurement, such as weak energy balance closure, low fluxes value in the night-time, etc.

Though field experiments were made only on the North China Plain and with single plant type of winter wheat, the model could be applied in other climatic regions and for other plant types. Therefore, the current experiments did not display the ability of the model fully. On the other hand, the model needs to be validated by more experiments in various regions and plants.

## RESULTS

### *Simulated net radiation, sensible and latent heat fluxes and soil heat flux*

The comparisons of simulated and measured half-hourly averaged net radiation, sensible heat flux, latent heat flux and soil heat flux during the whole growing season of winter wheat are shown in Figures 3 and 4 (similar figures omitted) and Table II. As shown in Figures 3 and 4 and Table II, simulated  $R_n$  was close to measured  $R_n$  except during January (ME = 0.73), indicating that

the model effectively simulated the transfer process of solar radiation above and inside the canopy. Simulated  $R_n$  was higher than the measured  $R_n$  in November, January and February and was lower than the measured  $R_n$  in March, April and May. This may have been caused by the decrease of canopy albedo for solar radiation with the growth of winter wheat, whereas the same albedo was used in the model during the whole growth period. Simulated soil heat flux agreed well with the measured soil heat flux except during January (ME = 0.46). Soil heat flux was estimated by soil temperatures at different depths in the model and, therefore, the accuracy of soil heat flux was determined by the accuracy of soil temperatures. Figure 5 shows the comparisons of simulated and measured soil temperatures at different depths from 1 to 15 April 2003. Soil temperatures were simulated reasonably well for this continuous period. Simulated latent heat fluxes did not agree well with measured ones, especially in November, January and February, when LAI is small. One of the main reasons for these errors was the energy imbalance observed in the agro-ecosystem, especially in the low LAI. The validation of the energy balance closure during the whole growth period is presented in Figure 6. The slope was less than unity during the whole growth period, ranging from 0.48 to 0.76, with a mean of 0.66, and the energy imbalance was smaller with the increase of LAI. The intercept ranged from 7.81 to 13.68 W m<sup>-2</sup>, with a mean value of 11.17 W m<sup>-2</sup>. The mean coefficient of determination  $R^2$  was 0.85, ranging from 0.67 to 0.95. Surface energy fluxes ( $H + \lambda E$ ) are underestimated by about 20–50% relative to the estimates of available energy ( $R_n - G$ ). On the other hand, the effect of atmospheric stability on energy exchange may contribute to the differences. When the atmosphere was in a stable condition, especially in the night-time, the vertical exchange processes were strongly reduced and the difference between the observation and modelling became larger, which suggests that the correction

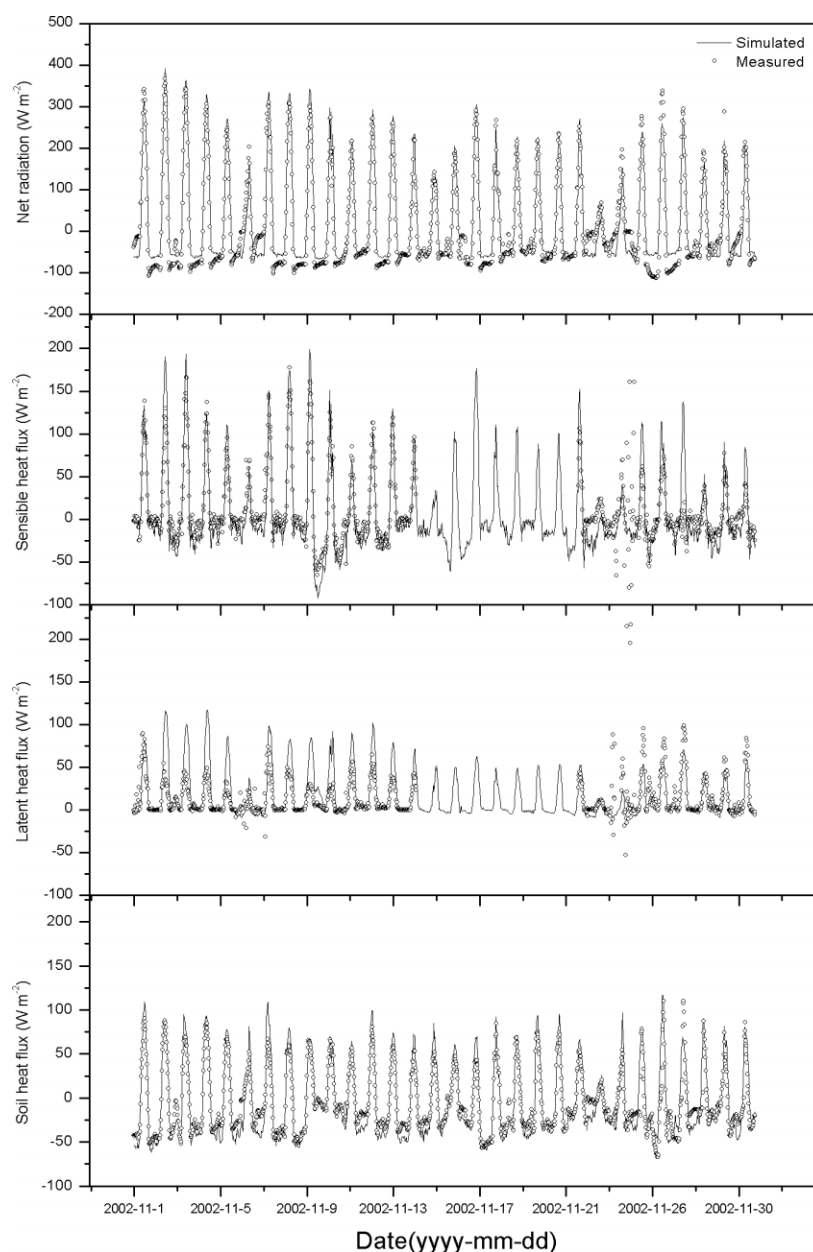


Figure 3. Measured and simulated components of the surface energy balance over the winter wheat canopy in Yucheng during 1–30 November 2002 (all fluxes are in  $\text{W m}^{-2}$  and assumed positive towards the surface)

method of the effect of atmospheric stability on turbulent exchange used in the model needs to be modified further. Even then, comparisons between the measured and simulated values show that the model did well in simulating the diurnal and seasonal variations of the components of energy when the energy imbalance was not evident.

#### *Simulation of carbon dioxide flux above the canopy*

Figure 7 shows a comparison of half-hourly, averaged simulated and measured  $\text{CO}_2$  fluxes above the winter wheat canopy. The simulated  $\text{CO}_2$  fluxes are in good agreement with measured values, with a small intercept of  $-0.017 \text{ mg m}^{-2} \text{ s}^{-1}$ . The slope was 0.87 and the correlation was typically good ( $R^2 = 0.87$ ). The errors may be due to the following reasons. The accuracy of modelled  $\text{CO}_2$  flux was strongly dependent on the modelled

photosynthetic active radiation absorbed by the canopy, which in turn related to modelled LAI, modelled photosynthetic active radiation above the canopy, and the process method on the structure of the canopy. In the model, the canopy was divided into sunlit leaves that intercepted direct and diffuse radiation and sunshaded leaves that only intercepted diffuse radiation; therefore, the determination of direct radiation and diffuse radiation was of importance in modelling photosynthetic active radiation absorbed by the canopy. The division of direct radiation and solar radiation was made according to an empirical function of solar radiation and inclination of the sun, which is most appropriate for a very clear day. However, this weather condition did not often occur. In the night-time,  $\text{CO}_2$  fluxes comprised dark respiration and soil respiration. In the model, dark respiration and soil respiration were taken as the functions only, independent

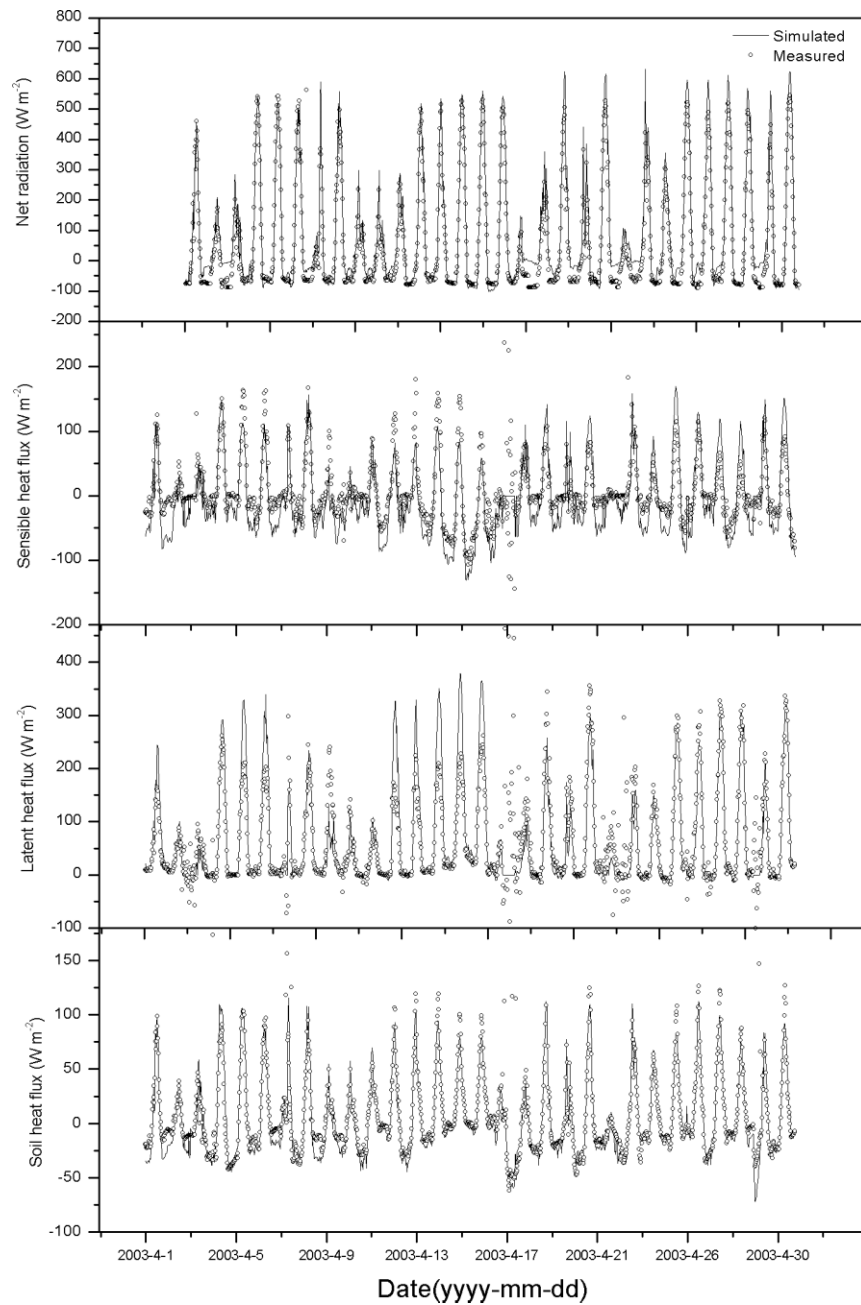


Figure 4. Measured and simulated components of the surface energy balance over the winter wheat canopy in Yucheng from 1 to 28 April 2003

Table II. The comparison of measured and simulated components of the surface energy balance over the growing season of winter wheat<sup>a</sup>

	Net radiation ( $W m^{-2}$ )			Latent heat flux ( $W m^{-2}$ )			Sensible heat flux ( $W m^{-2}$ )			Soil heat flux ( $W m^{-2}$ )		
	ME	RMSD	MBE	ME	RMSD	MBE	ME	RMSD	MBE	ME	RMSD	MBE
Nov	0.93	29.97	6.88	0.02	20.26	4.77	0.68	20.37	-2.77	0.81	15.53	1.35
Jan	0.73	49.53	14.97	0.27	20.22	-1.55	0.55	12.69	-1.79	0.46	27.83	8.41
Feb	0.93	30.51	0.20	0.14	17.36	2.24	0.81	17.87	-8.81	0.91	13.36	-1.90
Mar	0.95	32.38	-6.48	0.66	26.88	6.90	0.75	28.09	-9.65	0.89	13.78	-1.64
Apr	0.95	43.32	-26.68	0.77	39.34	1.27	0.57	30.43	-12.24	0.92	9.73	-1.52
May	0.93	58.09	-19.39	0.93	24.96	-0.65	0.44	28.65	0.33	0.66	19.34	-0.02

<sup>a</sup> The model efficiency  $ME = 1 - \frac{\sum_{i=1}^n (Y_o - Y_s)^2}{\sum_{i=1}^n (Y_o - \bar{Y})^2}$ ; the root-mean-square difference  $RMSD = [\sum_{i=1}^n (Y_o - Y_s)^2 / n]^{1/2}$ ; the mean bias error  $MBE = (1/n) \sum_{i=1}^n (Y_s - Y_o)$ , where  $Y_o$  is the observed value;  $Y_s$  is the simulated value;  $\bar{Y}$  is the mean of the observed values;  $n$  is the number of observations (Flerchinger and Hardegee, 2004).

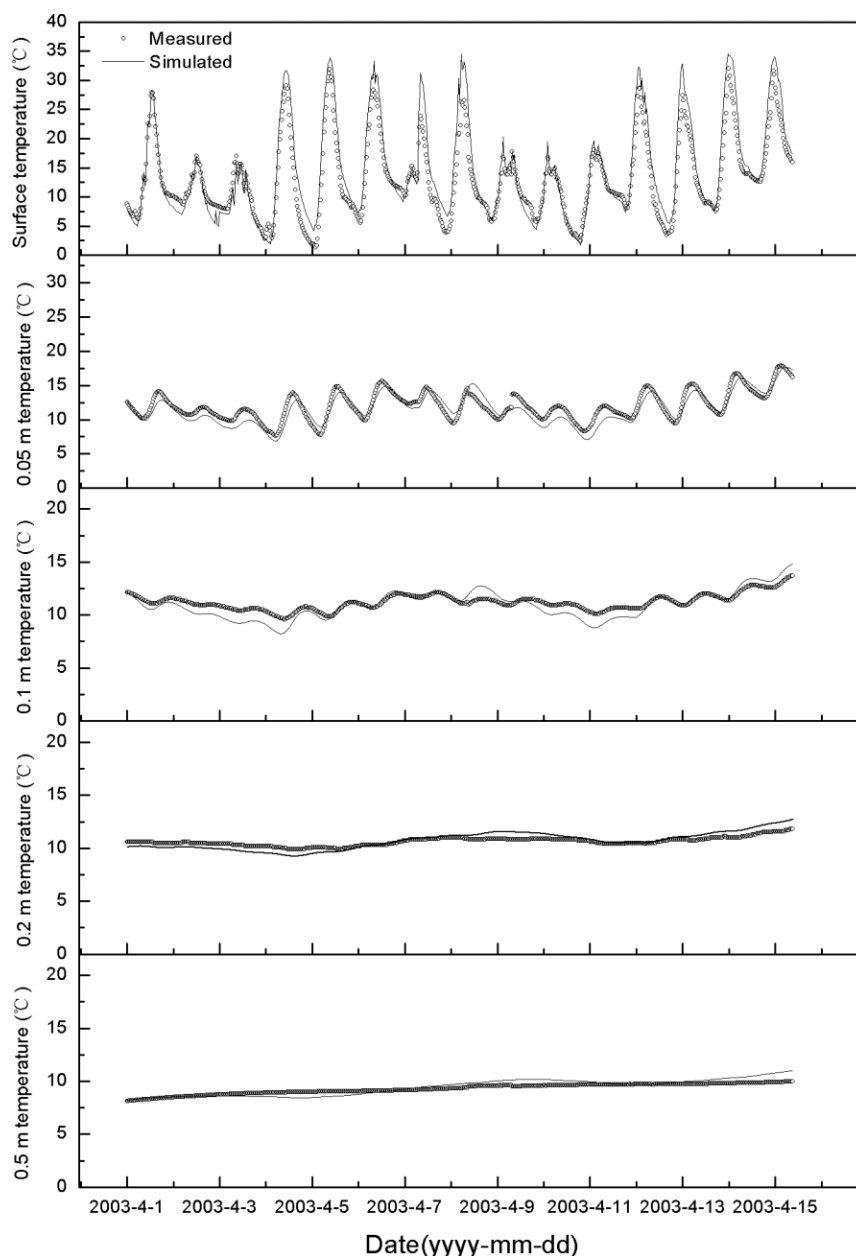


Figure 5. Measured and simulated soil temperatures at the surface and 0.05, 0.1, 0.2 and 0.5 m depths for 15 consecutive days in April 2003

of leaf temperature and soil temperature respectively, which is too simple and with values different from actual field conditions.

Midday depression of photosynthesis was a common phenomenon under natural conditions and was caused by both stomatal and non-stomatal elements. Leaf water potential in the period of water loss was higher than that in the period of water gain. The status of leaf water was determined by the balance between water loss through transpiration and the supply from the soil through absorption by roots. As transpiration was mainly determined by solar radiation and temperature, the leaf water potential responded mainly to solar radiation and air temperature. High solar radiation caused large decreases in leaf water potential. Owing to the accumulated effect of water loss from leaves, the leaf water potential reached its minimum

in the afternoon and would recover before sunset, when solar radiation was low. Midday depression of photosynthesis may occur due to stoma closure at low leaf water potential. The consideration of the dynamics of leaf water potential could raise the precision of simulation of  $\text{CO}_2$  and water vapour fluxes, especially in the afternoon under water stress conditions (Figure 8).

#### *Simulation of evapotranspiration*

The simulations of total evapotranspiration were made for three full growing cycles of winter wheat during 1998–2001 (Figure 9). The relative errors of measured and simulated accumulated evapotranspiration during the three growing seasons of winter wheat in 1998–1999, 1999–2000 and 2000–2001 are 0.4%, 0.7% and 2.7% respectively (Table III). The total evapotranspiration was

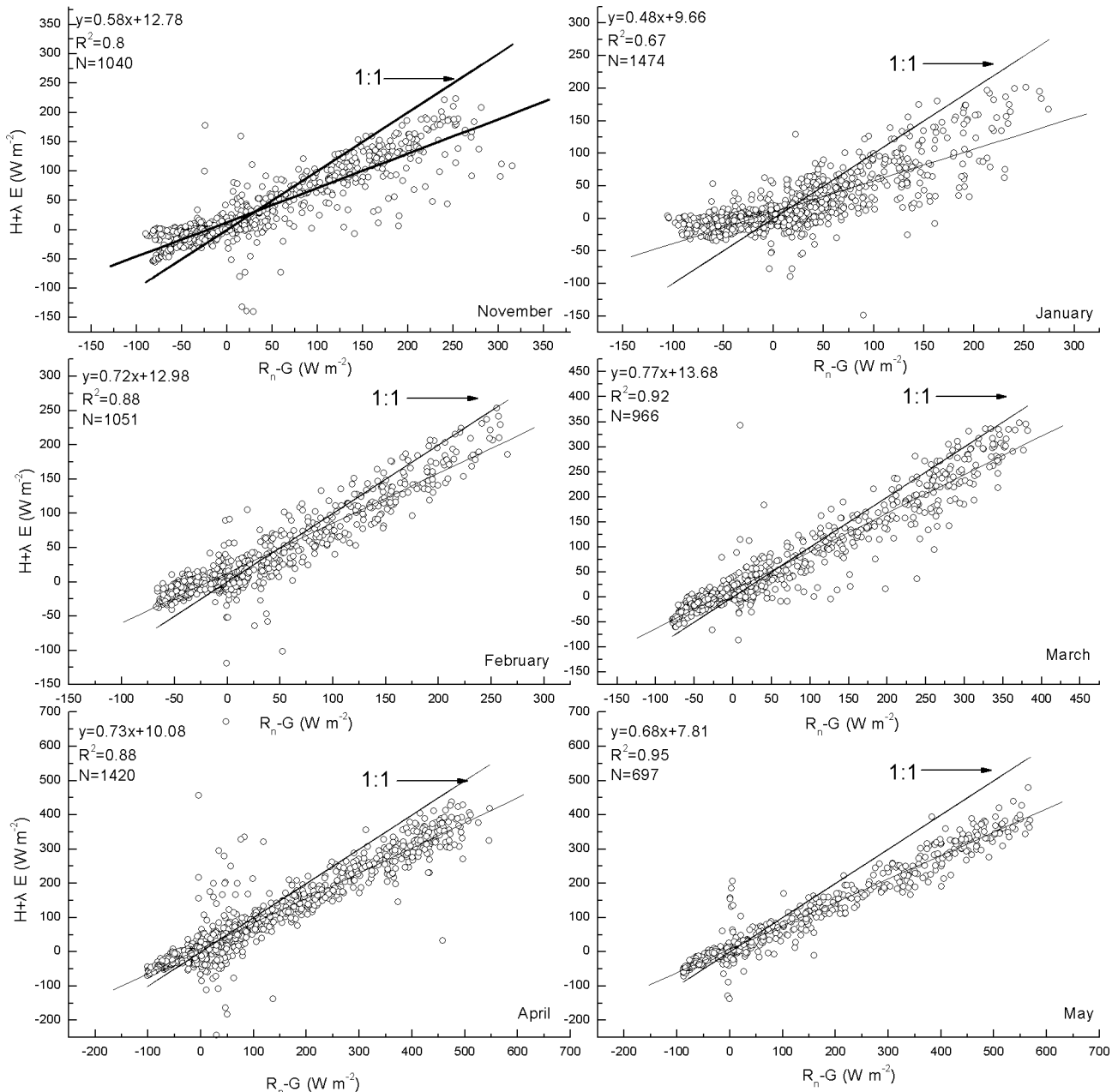


Figure 6. The energy-balance closure. The half-hourly average available energy ( $R_n - G$ ) plotted against the sum of the partitioning components ( $H + \lambda E$ ) during the growth period of winter wheat during 2002–2003

in reasonable agreement with the measured evapotranspiration. However, there were relatively larger errors between the daily simulated and the measured evapotranspiration, which were mainly caused by the redistribution of soil water after one precipitation or irrigation. Though the model could simulate the vertical movement of water in the soil, it did not consider the soil surface water evaporation, which was a very large value, especially after one violent precipitation or irrigation. Evapotranspiration stayed at less than 2.0 mm due to low air temperature and LAI, before the 'turning green' stage. With the increase of LAI and the rising of air temperature, evapotranspiration began to increase and reached a peak stage with an average value of 4.0 mm from the 'jointing' stage to the 'milky' stage.

#### Simulation of leaf area index

Accurate estimation of canopy photosynthesis and evapotranspiration depends strongly on the simulation of LAI. The comparison of simulated and measured LAI for winter wheat during the 2000–2001 and 2002–2003 growing seasons shows that the simulated LAI effectively followed the measurements (Figure 10). LAI stayed almost constant before turning green, and started to increase to its peak LAI during the heading stage and then fell sharply to zero. In the two growing seasons of winter wheat, peak LAIs were 6.40 and 4.22 respectively, which are representative of average LAIs in the growing season of winter wheat in the North China Plain. However, it may be noted that the function for simulating LAI in the model was very empirical and dependent

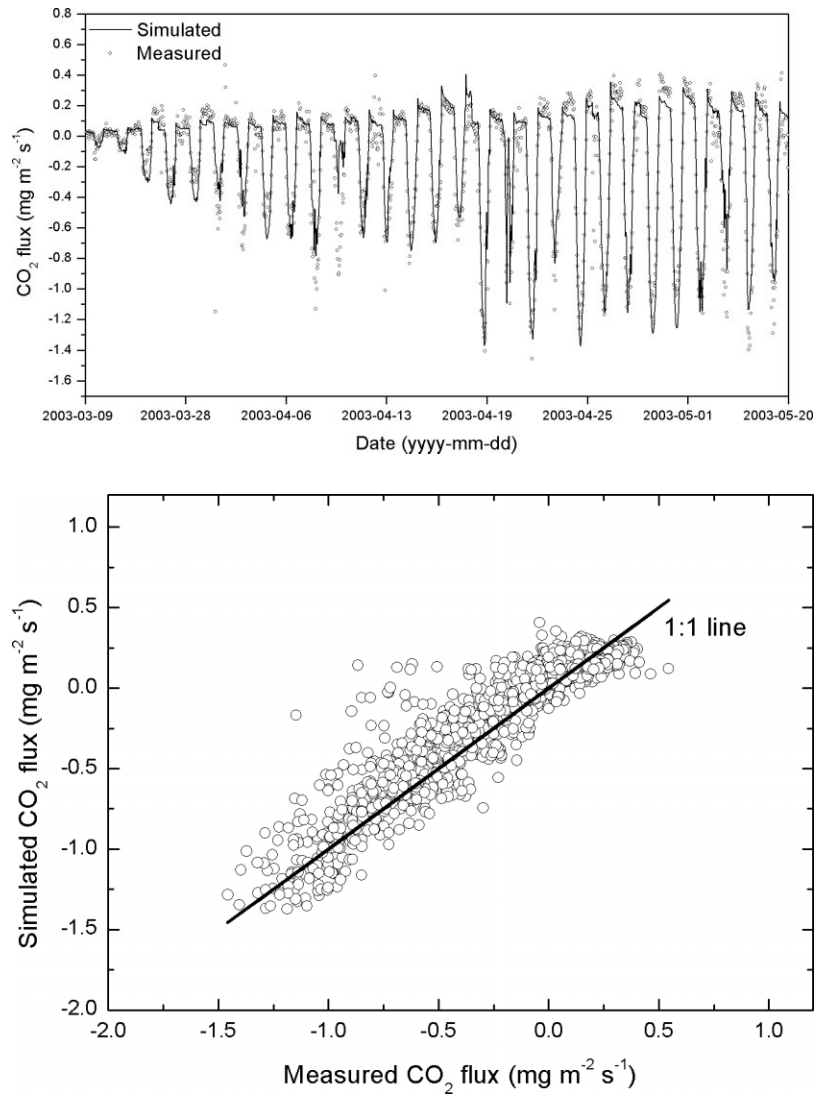


Figure 7. Measured and simulated CO<sub>2</sub> flux (mg m<sup>-2</sup> s<sup>-1</sup>) over the winter wheat canopy in Yucheng from 9 March to 20 May 2003 (discontinuous, some measured data missing)

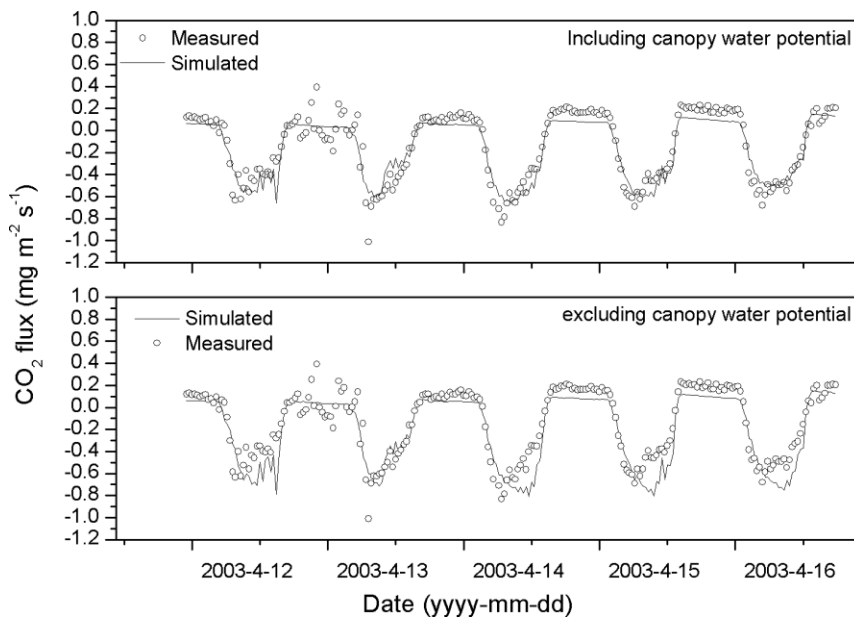


Figure 8. Influence of canopy water potential on simulated CO<sub>2</sub> flux

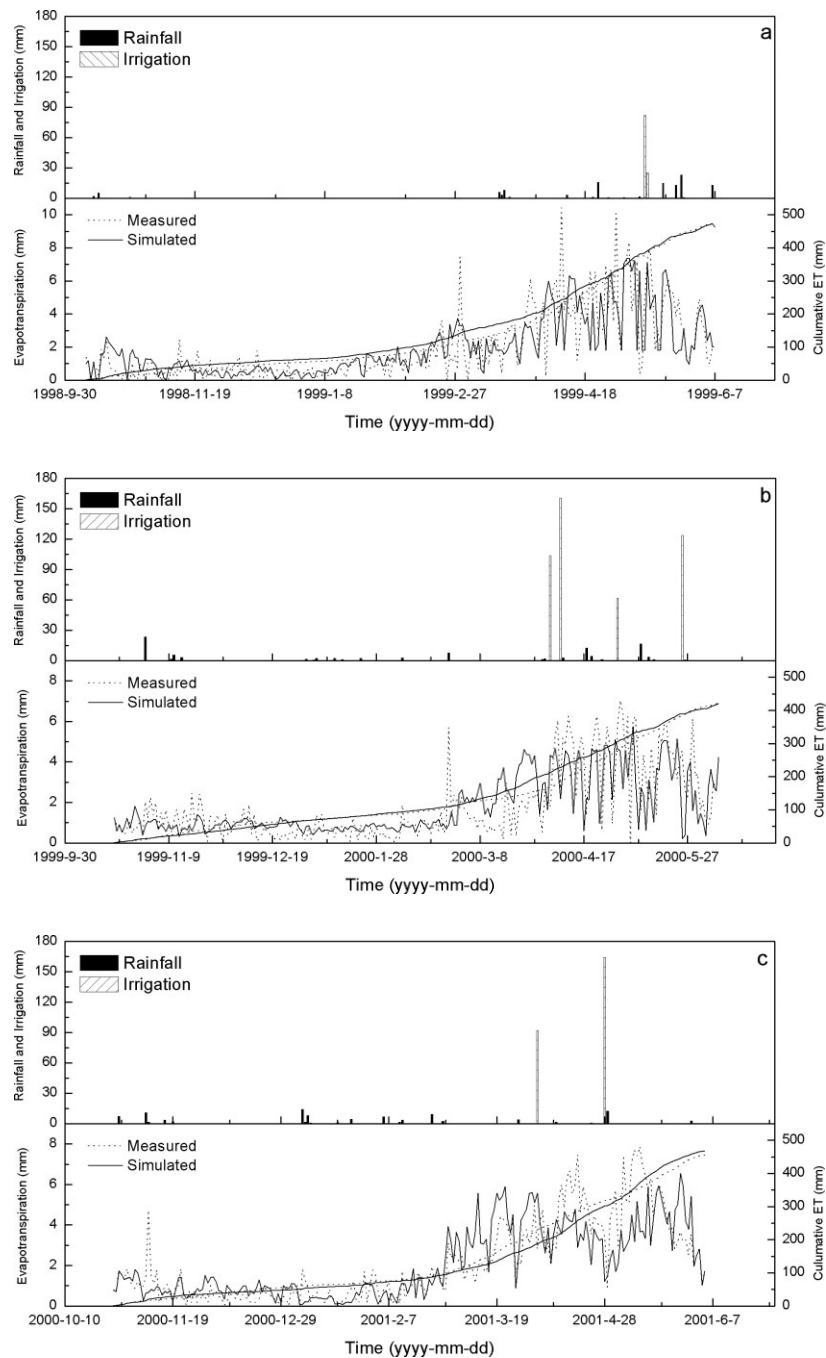


Figure 9. Simulated and measured evapotranspiration during 1998–1999, 1999–2000 and 2000–2001 for a winter-wheat growing season

Table III. Simulated and measured accumulated evapotranspiration during 1998–1999, 1999–2000 and 2000–2001 for the winter-wheat growing season

	Total evapotranspiration (mm)		
	1998–1999	1999–2000	2000–2001
Measured	464.8	424.0	468.6
Simulated	462.8	421.1	455.9

on some empirical parameters, such as specific leaf area ratio, maximal death rate of leaves, empirical partitioning coefficient of dry matter to leaves, etc., which limited the application of the model.

#### *Comparisons of simulated daily net ecosystem exchange and evapotranspiration under different time steps*

The time step was an important factor that a model had to take into account. If the time step is short, then the calculation may take a long time, which decreases the efficiency of the model. Furthermore, for shorter time steps the model includes more process and needs more input variables and parameters. However, if the time step is longer, then the model may ignore some important changes, which may cause large errors in simulated results. Figure 11 shows a comparison of simulated daily evapotranspiration and net ecosystem exchange (NEE) rates when the model ran under seven different time steps. We took 1 h as the basic time

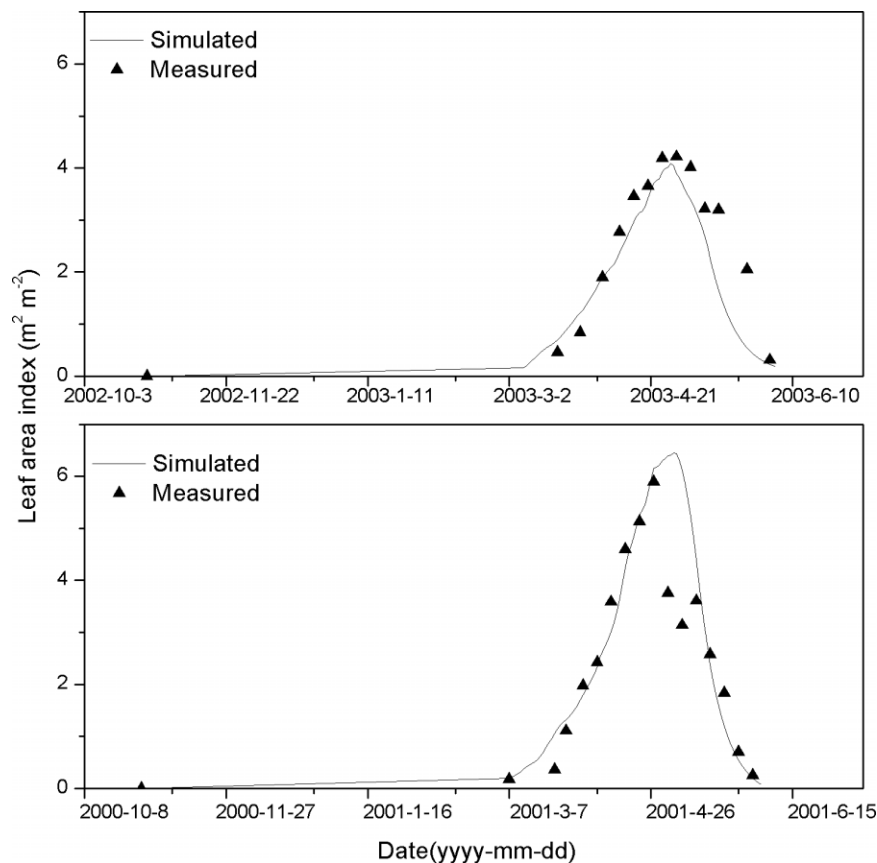


Figure 10. Simulated and measured LAI during the growing seasons of 2000–2001 and 2002–2003 for a winter-wheat growing season

step and then compared other simulated values with this basic value. The correlation analysis (Figure 12) indicates that there were no significant differences between the simulated daily evapotranspiration rates under different time steps. The slopes were 1.004, 0.986, 0.953, 0.980, 0.890 and 0.954, and the intercepts were 0, 0.015, 0.063, 0.016, 0.125 and 0.074 respectively. However, there were evidently different results in simulating the daily NEE. The value of a 1 h step NEE was close to the values of a 30 min step NEE, 2 h step NEE and 3 h step NEE. The slopes were 0.999, 1.006 and 1.005 respectively, and the intercepts were 0, 0.015 and 0.063 respectively. But when the time step increased to 4, 6 and 8 h, NEE was significantly different from that of the 1 h step NEE. The slopes were 0.936, 0.885 and 0.776 respectively, and the intercepts were 0.016, 0.125 and 0.074 respectively. This may be due to the difference between the calculated photosynthetic active radiations absorbed by the canopy when the model ran under different time steps.

## DISCUSSION AND CONCLUSIONS

It is unrealistic to consider all the interactions between the environment and crops in a soil–vegetation–atmosphere model as a result of the complexity of the system. Empirical models cannot really reflect the objective world; however, more mechanistic models require more inputs and parameters. Reaching a balance between the empirical

and the mechanistic is difficult, and it is also important to keep a balance between all the processes that are simulated by a model (Monteith, 1996). The characteristics of the ChinaAgrosys model are to keep a balance between the soil, plant and microclimate modules. The model does not oversimplify any biophysical and physiological processes within the soil–plant–atmosphere continuum (SPAC) in which photosynthesis and evapotranspiration are coupled by parameterization of canopy resistance. The concept of a modular structure is adopted in the model, and every module may be applied independently and can be substituted by a more advanced model.

The model presented in this paper combines energy and CO<sub>2</sub> flux transfers with crop growth and development, and it can simulate diurnal and seasonal variation of energy and CO<sub>2</sub> fluxes. This is based on an integrated photosynthesis, transpiration and stomatal-conductance model. The model is capable of predicting sound physiological responses to light, temperature, VPD, CO<sub>2</sub> and soil water. The photosynthesis model is simplified from a biochemical model. It can be specific for either the C<sub>3</sub> or the C<sub>4</sub> plant, and is easy to include the canopy energy-balance model to describe biophysical processes. Seasonal variations of energy partitioning and CO<sub>2</sub> releases depend strongly on LAI. Midday depression was caused by both stomatal and non-stomatal elements (Yu *et al.*, 2002). The transpiration is determined mainly by solar radiation and air temperature. High solar radiation and air temperature lead to high transpiration, which causes

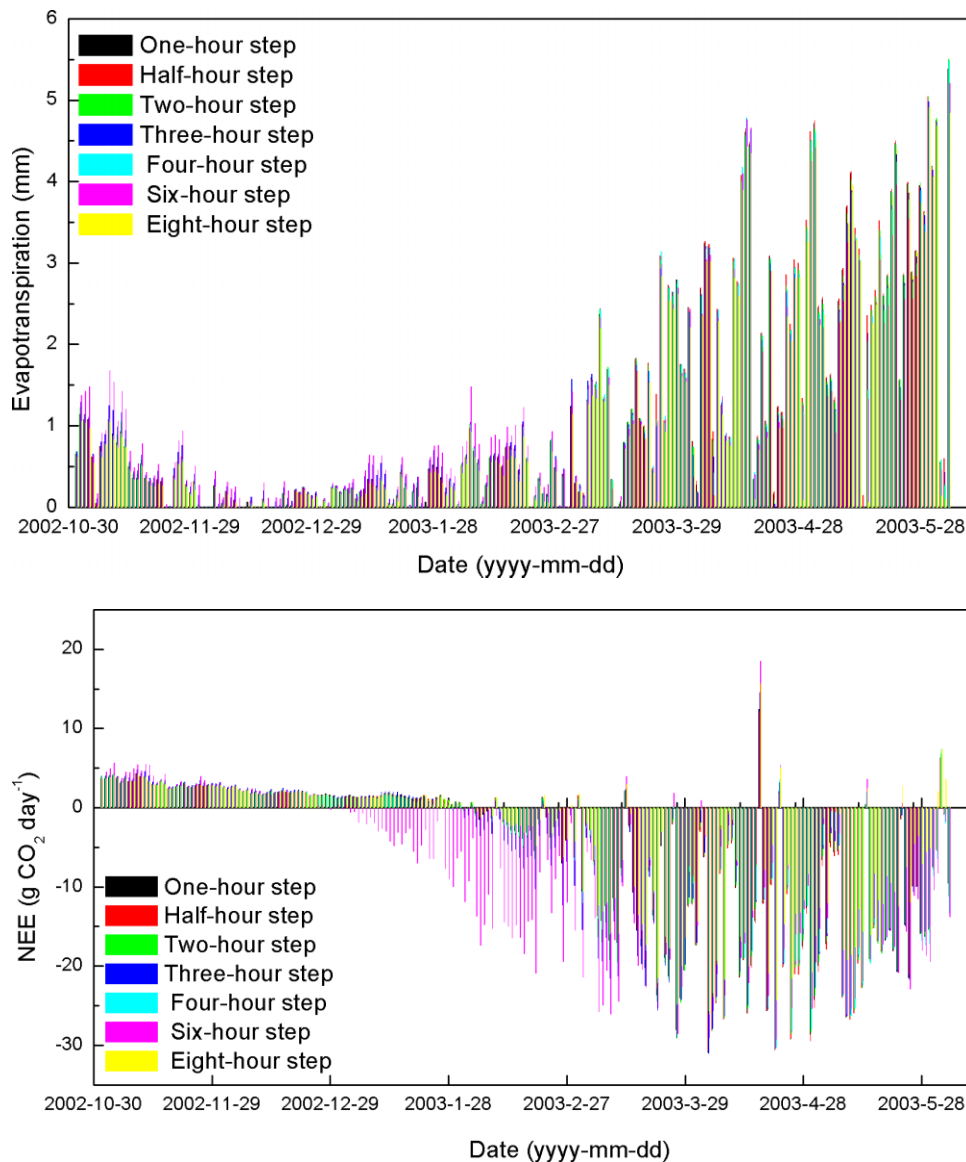


Figure 11. The comparison of simulated daily-integrated evapotranspiration and NEE for different time steps in 1999–2000

large decreases in canopy water potential. Owing to accumulated water loss from leaves, canopy water potential reaches its minimum in the afternoon, and it will recover before sunset, when solar radiation and air temperature are low. When canopy water potential is low, stomatal closure may occur and cause midday depression of photosynthesis. Consideration of the influence of canopy water potential in the photosynthesis model promotes an accurate simulation of CO<sub>2</sub> flux.

This paper is focused on the simulation of energy and CO<sub>2</sub> fluxes, as well as on changes in LAI. One of the important characteristics of the model is the simultaneous consideration of crop assimilation and water balances achieved by calculations made at short time steps (1 h or less) in order to capture the physiological responses of crop growth and water use as they respond to diurnal environmental patterns. Many crop-growth models take daily time steps to simulate canopy photosynthesis and evapotranspiration, such as CERES-Wheat, WOFOST and EPIC. However, there is a need for hourly time steps,

because the light-response curves of canopy photosynthesis are non-linear and the temperature-response curves of canopy photosynthesis have optima. Moreover, the midday depression of canopy photosynthesis may often occur. Therefore, an input of the average solar radiation and air temperature may be different from the average of the hourly values. Using longer time steps, such as daily or monthly ones, can simplify the modelling process and decrease the inputs of the models, but it may lose the resolution that is desired. However, multiple time-scales may make the models more complicated. Therefore, comparing the results under the different time steps and finding the controlling factor is of importance in simplifying the model in order to simulate the energy and CO<sub>2</sub> exchange between the vegetation and the atmosphere.

The model performs well in simulating water, heat and CO<sub>2</sub> fluxes, as well as crop growth and development. The model has important consequences for application in water resources management. It is a useful tool for studying the controlling factors of water, heat and CO<sub>2</sub>

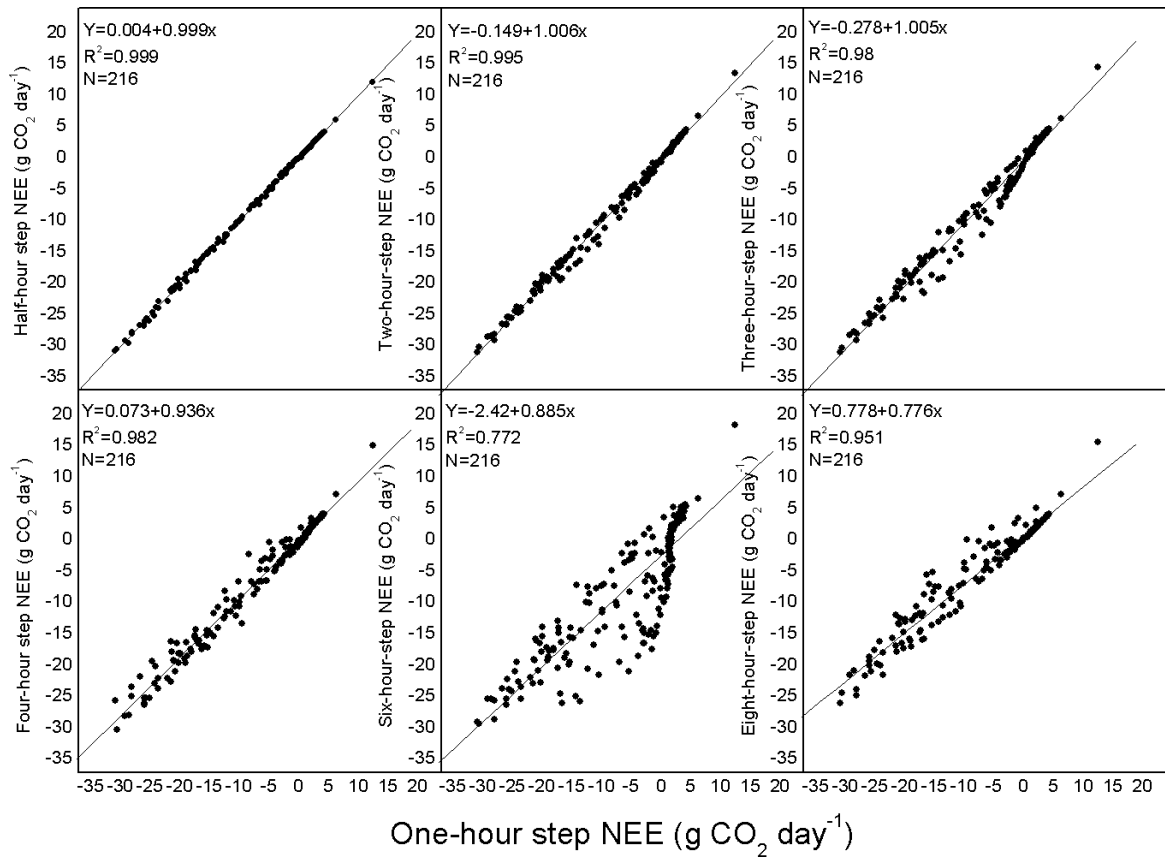
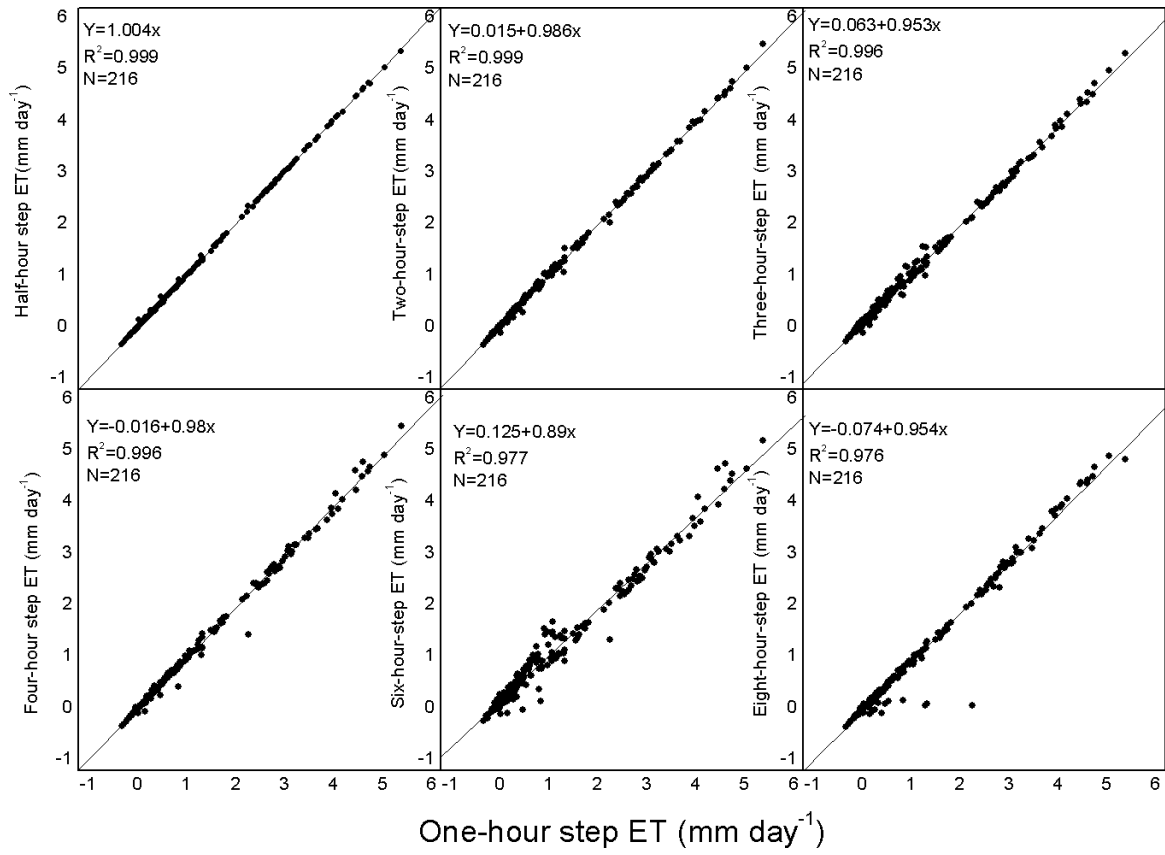


Figure 12. Correlations between simulated values under other time steps and 1 h step-simulated values

fluxes, and crop growth of the vegetation–atmosphere interaction. As the model is sound in the main feedback mechanisms in an agro-ecosystem, it is capable of making an impact on the evaluation of climate change on crop growth. In combination with an agricultural ecosystem model and with input from GCMs, this model could be used to study the interactions between crop and atmosphere.

## ACKNOWLEDGEMENTS

This work was supported by the Significant Item of Knowledge Innovation Project of the Chinese Academy of Science (KZCX1-SW-01-01A6) and the National Natural Science Foundation of China (no. 40328001). We thank Professor Tianduo Wang (Shanghai Institute of Plant Physiology and Ecology, Chinese Academy of Sciences) and Dr Flerchinger (USDA-ARS) for their helpful comments on this paper.

## REFERENCES

- Arora VK, Gajri PR. 2000. Assessment of a crop growth–water balance model for predicting maize growth and yield in a subtropical environment. *Agricultural Water Management* **46**: 157–166.
- Avissar R, Avissar P, Mahrer Y, Bravdo BA. 1985. A model to simulate response of plant stomata to environmental conditions. *Agricultural and Forest Meteorology* **34**: 21–29.
- Baldocchi D. 2003. Assessing the eddy covariance technique for evaluating carbon dioxide exchange rates of ecosystems, past, present and future. *Global Change Biology* **9**: 479–492.
- Ball JT, Woodrow IE, Berry JA. 1987. A model predicting stomatal conductance and its contribution to the control of photosynthesis under different environmental conditions. In *Progress in Photosynthesis Research*, Biggins I (ed.). Martinus Nijhoff: the Netherlands; 221–224.
- Bonan GB. 1995. Land–atmosphere interactions for climate system models, coupling biophysical, biogeochemical, and ecosystem dynamical processes. *Remote Sensing of Environment* **51**: 57–73.
- Bonan GB. 1996. *The NCAR land surface model (LSM version 1-0) coupled to the NCAR community climate model*. Technical Report NCAR/TN-429 + STR, NCAR Boulder, CO.
- Boons-Prins ER, de Koning GHJ, van Diepen CA, Penning de Vries FWT. 1993. *Crop specific simulation parameters for yield forecasting across the European community*. Simulation Reports CABO-TT, no. 32.
- Braden H. 1995. *The model AMBETI. A detailed description of a soil–plant–atmosphere model*. Berichte des Deutschen Wetterdienstes Nr. 195, Offenbach am Main.
- Braud I, Dantas-Antonino AC, Vauclin M, Thont JL, Ruelle P. 1995. A simple soil–plant–atmosphere transfer model (SiSPAT) development and field verification. *Journal of Hydrology* **166**: 213–250.
- Brenner AJ, Incoll LD. 1997. The effect of clumping and stomatal response on evaporation from sparsely vegetated shrub lands. *Agricultural and Forest Meteorology* **84**: 187–205.
- Charney JG. 1975. Dynamics of deserts and drought in the Sahel. *Quarterly Journal of the Royal Meteorological Society* **101**: 193–202.
- Chen J. 1984a. Uncoupled multi-layer model for the transfer of sensible and latent heat flux densities from vegetation. *Boundary-Layer Meteorology* **28**: 213–225.
- Chen J. 1984b. *Mathematical analysis and simulation of crop micrometeorology*. PhD thesis, Department of Theoretical Production Ecology, Agricultural University, Wageningen, the Netherlands.
- Choudhury BJ, Monteith JL. 1988. A four-layer model for the heat budget of homogenous land surfaces. *Quarterly Journal of the Royal Meteorological Society* **114**: 373–398.
- Choudhury BJ, Reginato RJ, Idso SB. 1986. An analysis of infrared temperature observations over wheat and calculation of latent heat flux. *Agricultural and Forest Meteorology* **37**: 75–88.
- Collatz GJ, Ball JT, Grivet C, Berry JA. 1991. Physiological and environmental regulation of stomatal conductance, photosynthesis and transpiration: a model that includes a laminar boundary layer. *Agricultural and Forest Meteorology* **54**: 107–136.
- Cox P, Betts R, Jones C, Spall S, Totterdell I. 2000. Acceleration of global warming due to carbon-cycle feedbacks in a coupled climate model. *Nature* **408**: 184–187.
- Dawes W, Hatton TJ. 1993. *TOPOG-IRM. 1. Model description*. Division of Water Resources Technical Memorandum 93/5. CSIRO, Canberra.
- Deardorff JW. 1978. Efficient prediction of ground surface temperature and moisture with inclusion of a layer of vegetation. *Journal of Geophysical Research* **83**: 1889–1903.
- Dickinson RE. 1984. Modelling evapotranspiration for three-dimensional global climate models. *Geophysical Monograph* **29**: 58–72.
- Dickinson RE. 1995. Land processes in climate models. *Remote Sensing of Environment* **51**: 27–38.
- Dickinson RE, Henderson-Sellers A. 1988. Modelling tropical deforestation: a study of GCM land-surface parameterizations. *Quarterly Journal of the Royal Meteorological Society* **114**: 439–462.
- Dickinson RE, Henderson-Sellers A, Rosenzweig C, Wilson PF. 1986. *Biosphere-Atmosphere-Transfer-Scheme (BATS) for the NCRA Community Climate Model*. National Center for Atmospheric Research Note, NCAR/TN-275.
- Dickinson RE, Shaikh M, Bryant R, Graumlich L. 1998. Interactive canopies for a climate model. *Journal of Climate* **11**: 2823–2836.
- Dirnmer PA, Shukla J. 1994. Albedo as a modulator of climate response to tropical deforestation. *Journal of Geophysical Research* **99**: 863–877.
- Dolman AJ. 1993. A multiple source land surface energy balance model for use in GCMs. *Agricultural and Forest Meteorology* **65**: 2–45.
- Dolman AJ, Gash JHC, Goutorbe JP, Kerr Y, Lebel T, Prince SD, Stricker JNM. 1997. The role of the land surface in Sahelian climate: HAPEX-Sahel results and future research needs. *Journal of Hydrology* **188–189**: 1067–1079.
- Famiglietti J, Wood E. 1994. Multiscale modeling of spatially variable water and energy balance processes. *Water Resource Research* **30**: 3061–3078.
- Farquhar GD, von Caemmerer S, Berry JA. 1980. A biochemical model of photosynthetic CO<sub>2</sub> assimilation in leaves of C<sub>3</sub> species. *Planta* **149**: 78–90.
- Flerchinger GN, Hardegree SP. 2004. Modelling near-surface soil temperature and moisture for germination response predictions of post-wildfire seedbeds. *Journal of Environment* **59**: 369–385.
- Flerchinger GN, Pierson FB. 1991. Modeling plant canopy effects on variability of soil temperature and water. *Agricultural and Forest Meteorology* **56**: 227–246.
- Flerchinger GN, Saxton KE. 1989. Simultaneous heat and water model of a freezing snow-residue–soil system: I. Theory and development. *Transactions of the ASAE* **32**: 573–578.
- Goudriaan J. 1977. *Crop Micrometeorology: A Simulation Study*. Center for Agricultural Publishing and Documentation: Wageningen, the Netherlands.
- Goudriaan J. 1996. Predicting crop yields under global change. In *Global change and terrestrial ecosystems*, Walker BH, Steffen W (eds). Cambridge University Press: Cambridge.
- Goudriaan J, van Laar HH. 1994. *Modelling Potential Crop Growth Processes: Textbook with Exercises*. Kluwer: Dordrecht.
- Harley PC, Baldocchi DD. 1995. Scaling carbon dioxide and water vapor exchange from leaf to canopy in a deciduous forest: leaf level parameterization. *Plant Cell and Environment* **18**: 1146–1156.
- Harley PC, Thomas RB, Reynolds JF, Strain BR. 1992. Modelling photosynthesis of cotton grown in elevated CO<sub>2</sub>. *Plant Cell and Environment* **15**: 271–282.
- Hillel D, Talpaz H, Van Keulen. 1976. A macroscopic-scale model of water uptake by a non-uniform root system and of water and salt movement in the soil profile. *Soil Science* **121**: 242–255.
- Hirasawa T, Hsiao TC. 1999. Some characteristics of reduced leaf photosynthesis at midday in maize growing in the field. *Field Crops Research* **62**: 53–62.
- Hoogenboom G. 2000. Contribution of agrometeorology to the simulation of crop production and its applications. *Agricultural and Forest Meteorology* **103**: 137–157.
- Jacobs CMJ, van den Hurk BJJM, de Bruin HAR. 1996. Stomatal behavior and photosynthetic rate of unstressed grapevines in semi-arid conditions. *Agricultural and Forest Meteorology* **80**: 111–134.
- Jarvis PG. 1976. The interpretation of leaf water potential and stomatal conductance found in canopies in the field. *Philosophical Transactions of the Royal Society of London, Series B: Biological Sciences* **273**: 593–610.

- Kustas WP. 1990. Estimations of evapotranspiration with one and two-dimension model of heat transfer over partial canopy cover. *Journal of Applied Meteorology* **29**: 704–715.
- Kustas WP, Norman JM. 1999. Evaluation of soil and vegetation heat flux predictions using a simple two-source model with radiometric temperatures for partial canopy cover. *Agricultural and Forest Meteorology* **94**: 13–29.
- Lean J, Rowntree PR. 1993. A GCM simulation of the impact of Amazonian deforestation on climate change using an improved canopy representation. *Quarterly Journal of the Royal Meteorological Society* **119**: 509–530.
- Lean J, Rowntree PR. 1997. Understanding the sensitivity of a GCM simulation of Amazonian deforestation to the specification of vegetation and soil characteristics. *Journal of Climate* **10**: 1216–1235.
- Lee X, Yu Q, Sun XM, Liu JD, Min QW, Liu YF, Zhang XZ. 2004. Micrometeorological fluxes under the influence of regional and local advection: a revisit. *Agricultural and Forest Meteorology* **122**: 111–124.
- Leuning R. 1995. A critical appraisal of a combined stomatal-photosynthesis model for C<sub>3</sub> plants. *Plant Cell and Environment* **18**: 339–355.
- Lin JD, Sun SF. 1983. A study of moisture and heat transport in soil and the effect of surface resistance to evaporation. *Journal of Hydraulic Engineering* **7**: 1–8 (in Chinese).
- Lu L, Pielke RA, Liston GE, Parton WJ, Ojima D, Hartman M. 2001. Implementation of a two-way interactive atmospheric and ecological model and its application to the central United States. *Journal of Climate* **14**: 900–919.
- Mall RK, Lal M, Bhatia VS, Rathore LS, Ranjeet S. 2004. Mitigating climate change impact on soybean productivity in India: a simulation study. *Agricultural and Forest Meteorology* **121**: 113–125.
- Mihailovic DT, Ruml M. 1996. Design of land–air parameterization scheme (LAPS) for modelling boundary layer surface processes. *Meteorology and Atmospheric Physics* **58**: 65–81.
- Monteith JL. 1965. Evaporation and environment. *Symposia of the Society of Experimental Biology* **19**: 205–234.
- Monteith JL. 1973. *Principles of Environmental Physics*. Edward Arnold: London.
- Monteith JL. 1996. The quest for balance in crop modelling. *Agronomy Journal* **88**: 695–697.
- Nikolov NT, Massman WJ, Schoettle AW. 1995. Coupling biochemical and biophysical processes at the leaf level: an equilibrium photosynthesis model for leaves of C<sub>3</sub> plants. *Ecological Modelling* **80**: 205–235.
- Noilhan J, Mahfouf JF. 1996. The ISBA land surface parameterization scheme. *Global and Planetary Change* **13**: 145–159.
- Noilhan J, Planton S. 1989. A simple parameterization of land surface processes for meteorological models. *Monthly Weather Review* **117**: 536–549.
- Nonhebel S. 1994. Inaccuracies in weather data and their effects on crop growth simulation results. I. Potential production. *Climate Research* **4**: 47–60.
- Nonhebel S. 1996. Effects of temperature rise and increase in CO<sub>2</sub> concentration on simulated wheat yields in Europe. *Climatic Change* **34**: 73–90.
- Penman HL. 1948. Natural evaporation from open water, bare soil and grass. *Proceedings of the Royal Society* **193**: 120–145.
- Penning de Vries FWT, Jansen DM, Ten Berge HFM, Bakema A. 1989. *Simulation of ecophysiological processes of growth in several annual crops*. Simulation Monographs 29, Pudoc, Wageningen.
- Priestley CHB, Taylor RJ. 1972. On the assessment of surface heat flux and evaporation using large-scale parameters. *Monthly Weather Review* **100**: 81–92.
- Puech-Suanzes I, Hsiao TC, Fereres E, Henderson DW. 1989. Water stress effects on the carbon exchange rates of three upland cotton (*Gossypium hirsutum* L.) cultivars in the field. *Field Crops Research* **21**: 239–255.
- Sellers PJ, Mintz Y, Sud YC, Dalcher A. 1986. A simple biosphere model (SiB) for use within general circulation models. *Journal of the Atmospheric Sciences* **43**: 505–531.
- Sellers PJ, Randall DA, Collatz GJ, Berry JA, Field CB, Dazlich DA, Zhang C, Collelo GD, Bounoua L. 1996. A revised land surface parameterization (SiB2) for atmospheric GCMs. Part I: model formulation. *Journal of Climate* **9**: 676–705.
- Shuttleworth WJ, Gurney RJ. 1990. The theoretical relationship between foliage temperature and canopy resistance in a sparse crop. *Quarterly Journal of the Royal Meteorological Society* **116**: 498–519.
- Shuttleworth WJ, Wallace JS. 1985. Evaporation from sparse crops—an energy combination theory. *Quarterly Journal of the Royal Meteorological Society* **111**: 839–855.
- Trivedi PK, Reddy MSS, Prafullachandra V. 2000. Plastid gene expression is not associated with midday depression in CO<sub>2</sub> assimilation and electron transport. *Plant Science* **155**: 187–192.
- Tsvetinskaya E, Mearns LO, Easterling W. 2001. Investigating the effect of seasonal plant growth and development in 3-dimensional atmospheric simulations. Part I: simulation of surface fluxes over the growing season. *Journal of Climate* **14**: 692–709.
- Van den Honert TH. 1948. Water transport in plants as a catenary process. *Discussion of the Faraday Society* **3**: 146–153.
- Van Keulen H, Penning de Vries FWT, Drees EM. 1982. A summary model for crop growth. In *Simulation of Plant Growth and Crop Production*, Penning de Vries FWT, van Laar HH (eds). Simulation Monographs. Pudoc: Wageningen.
- Verhoef A, Allen SJ. 2000. A SVAT scheme describing energy and CO<sub>2</sub> fluxes for multi-component vegetation: calibration and test for a Sahelian savannah. *Ecological Modelling* **127**: 245–267.
- Waggoner PE, Reifsnnyder WE. 1968. Simulation of the temperature, humidity and evaporation profiles in a leaf canopy. *Journal of Applied Meteorology* **7**: 400–409.
- Wang E, Engel T. 1998. Simulation of phenological development of wheat crops. *Agricultural Systems* **58**: 1–24.
- Wang J, Yu Q, Li J, Li LH, Li XG, Yu GR, Sun XM. 2006. Simulation of diurnal variations of CO<sub>2</sub>, water and heat fluxes over winter wheat with a model coupled photosynthesis and transpiration. *Agricultural and Forest Meteorology* **137**: 194–219.
- Wang YP, Leuning R. 1998. A two-leaf model for canopy conductance, photosynthesis and partitioning of available energy I. Model description and comparison with a multi-layered model. *Agricultural and Forest Meteorology* **91**: 89–111.
- Wolf J. 1993. Effects of climate change on wheat and maize production potential in the EC. In *The effect of climate change on agricultural and horticultural potential in Europe*, Kenny GJ, Harrison PA, Parry ML (eds). Research Report No. 2, Environmental Change Unit, University of Oxford: Oxford; 93–120.
- Xue Y. 1997. Biosphere feedback on regional climate in tropical North Africa. *Quarterly Journal of the Royal Meteorological Society* **123**: 1483–1515.
- Yu Q, Liu YF, Liu JD, Wang TD. 2002. Simulation of leaf photosynthesis of winter wheat on Tibetan Plateau and in North China Plain. *Ecological Modelling* **155**: 205–216.